Electronic Supplementary Material (ESI) for ChemComm.
This journal is © The Royal Society of Chemistry 2016

Supporting Information

General Procedures

All precursors were obtained from commercial suppliers and used without further purification. All reactions were performed under inert gas using Schlenk techniques. NMR measurements (^{1}H, ^{13}C, and ^{31}P) were performed on a JEOL 400 MHz spectrometer. Chemical shifts are reported as δ values (ppm) relative to TMS (^{1}H, ^{13}C) as the internal standard. ^{31}P NMR spectra were recorded at 121 MHz with 85% H_3PO_4 as an external reference. The type of signal is abbreviated as follows: s = singlet, d = doublet, t = triplet, q = quartet, dd = doublet of doublets, and m = multiplet. High-resolution mass spectra were measured using FTMS + p APCI or FTMS + p NSI (OrbitrapXL) at the University of Münster. Elemental analyses were performed at Analytical Laboratories, Prof. Dr. H. Malissa and G. Reuter GmbH, Germany. The geometric and electronic characteristics of all compounds (**1a**, **1b**, **2a**, **2b**), radical cations (**2a**$^{\bullet+}$, **2b**$^{\bullet+}$), dimers, trimers, tetramers, and their cations, were studied by DFT calculations at the B3LYP/6-311G** level of theory. The calculations on the system **2a-Au** were performed at the PBE1PBE using the LANL2DZ basis set for gold (Au) and 6-311G** on other atoms. The obtained structural and electronic parameters from ab initio calculations of all systems (Gaussian 09) agree well with the geometric and optical data from single crystal X-ray diffraction and UV-Vis spectroscopy, confirming the suitability of the employed DFT functional. All electrochemical experiments were carried out in a glovebox (MBraun) maintained with < 0.1 ppm levels of O_2 and H_2O. Cyclic voltammetry experiments were performed in a three-electrode electrochemical cell with glassy carbon or FTO glass as the working electrode, a glassy carbon rod as the counter electrode and $Ag/AgNO_3$ (10 mM/MeCN) as the reference electrode. Typically, 4 mg of sample were dissolved in 5 mL of 0.1 M *n*-Bu_4NPF_6 / DCM. The film growth was made by repetitive scans (*e.g.* 30 scans) in the 0 V to 1.3 V range at a scan rate of 100 mV s^{-1}; all the films were thoroughly washed with DCM and let dry prior to use. Spectroelectrochemistry experiments were performed in a three-electrode electrochemical cell with a polymer film coated FTO glass as working electrode, glassy carbon counter electrode and $Ag/AgNO_3$ (10 mM/MeCN) as reference electrode. The electrochemical cell was set up in a quartz cuvette with an optical pathway of 1 cm. The sample was immersed in 2 mL of 0.1 mM *n*-Bu_4NPF_6 DCM supporting electrolyte solution. The counter electrode was kept separate from the main solution by a salt bridge with a glass frit tip. All electrochemical measurements were performed using an Autolab PGSTAT302 potentiostat/galvanostat with a GPES electrochemical interface, while the spectra were acquired with an Agilent 8453 UV-Vis spectrophotometer. Scanning Electron Microscopy and Energy Dispersed X-ray Spectroscopy: Polymer films on conducting FTO glass substrate were transferred to conductive carbon tape on a sample holder disk, and coated using an Au/Pd-sputter coating for 30 sec. A Zeiss 1550 with AZtec EDS instrument was used for acquiring images using a 5 kV energy source under vacuum. Oxford EDS and Inca software for X-

ray mapping was used to analyse the elemental composition. **XPS General & Characterization Procedures are found in Page S15**. Synthesis of ***poly*-2a-AuCl**: In a dry glovebox (MBraun) (< 0.1 ppm levels of O_2 and H_2O), a vial containing chlorido(tetrahydrothiophene)gold(I) (16 mg) in acetonitrile (~3 mL) was heavily swirled until the gold complex dissolved, then, a film of ***poly*-2a** was placed into the vial, which was tightly capped and left reacting/diffusing in the glovebox for 3 weeks to yield ***poly*-2a-AuCl**.

Experimental

Synthetic Work

Synthesis of (2,7-dibromo-9H-fluoren-9-ylidene)(2,4,6-tri-tert-butylphenyl)phosphane (**1a**)

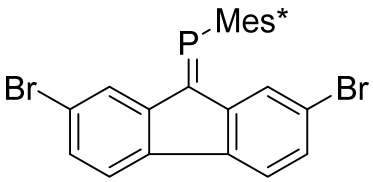

Same Procedure used in the synthesis of **1b** (PCl_3 was used instead) led to yellow crystals in 80% yield. ^{1}H NMR ($CDCl_3$, 400 MHz) δ (ppm): 8.34 (s, 1H), 7.60 (s, 2H), 7.44 (s, 2H), 7.37 (d, *J = 8 Hz*), 7.27 (s, 2H), 5.39 (s, 1H), 1.46 (s, 9H), 1.41 (s, 18H). ^{13}C NMR ($CDCl_3$, 125 MHz) δ (ppm): δ 166.6 (d, $^1J_{CP}$ = 45 Hz, P=C), 154.2 (*o*-Mes*), 152.47 (*p*-Mes*), 144.7 (d, $^2J_{CP}$ = 28 Hz, Ar), 139.50 (d, $^2J_{CP}$ =17 Hz, Ar), 137.17 (d, J_{CP} =10 Hz, Ar), 136.0 (d, J_{CP} =14 Hz, Ar), 132.82 (d, $^1J_{CP}$ = 56 Hz, *i*-Mes*), 131.05 (d, J_{CP} = 6 Hz, Ar), 130.89 (d, J_{CP} = 7 Hz, Ar), 129.42 (d, J_{CP} = 7 Hz, Ar), 123.66 (d, $^3J_{CP}$ = 24 Hz, Ar), 123.11 (*m*-Mes*), 121.20 (d, J_{CP} = 4 Hz, Ar), 121.03 (d, J_{CP} = 4 Hz, Ar), 120.87 (Ar), 120.32 (d, J_{CP} = 3 Hz, Ar), 38.39 (*t*-Bu), 35.40 (*t*-Bu), 32.92 (d, *J* = 7 Hz, *t*-Bu), 31.69 (*t*-Bu). ^{31}P NMR ($CDCl_3$, 121 MHz,) δ (ppm): 273.65. HRMS (FTMS + p APCI, toluene): 599.09000 m/z $[M+H]^+$ (calcd for $C_{31}H_{35}Br_2P$+H: 599.09009). Anal. Calcd for $C_{31}H_{35}Br_2P$ (%): C, 62.22; H, 5.90. Found: C, 62.21; H, 5.95. UV/Vis/NIR (DCM): λ_{max} (***ε***) = 276 nm (32 800 $M^{-1}cm^{-1}$), 286 nm (43 800 $M^{-1}cm^{-1}$) 371 nm (19 300 $M^{-1}cm^{-1}$).

Synthesis of (2,7-di(thiophen-2-yl)-9H-fluoren-9-ylidene)(2,4,6-tri-tert-butylphenyl)phosphane (**2a**)

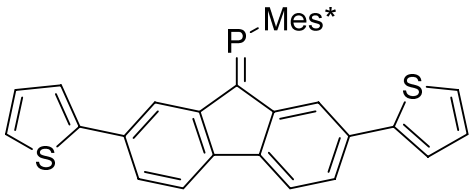

Same procedure used in the synthesis of **2b** led to a red-violet solid in 40% yield. ^{1}H NMR ($CDCl_3$, 400 MHz) δ (ppm): 8.50 (d, *J* = 4.5 Hz, 1H), 7.63 (m, 4H), 7.54 (s, 1H), 7.47 (dd, *J* = 8 Hz, 1.2 Hz, 1H), 7.41 (d, *J* = 8 Hz, 1H), 7.31 (dd, *J* = 8 Hz, 1.1 Hz, 1H), 7.14 (m, 2H), 6.95 (m, 1H), 6.76 (dd, *J* = 8 Hz, 1.2 Hz, 1H), 6.34 (s, 1H), 1.48 (s, 18H), 1.41 (s, 9H). ^{13}C NMR ($CDCl_3$, 100 MHz) δ = 167.73 (d, J_{CP} = *44 Hz)*, 154.26, 151.46, 144.93 (d, J_{CP} = 4 Hz), 144.26, 143.99, 139.49 (d, J_{CP} = 17 Hz), 138.37 (d, J_{CP} = 10 Hz), 136.90 (d, J_{PC} = 14 Hz), 133.93, 133.33, 132.80 (d, J_{PC} = 3 Hz), 128.08 (d, J_{CP} = *14 Hz*), 126.48 (d, J_{CP} = 6 Hz), 126.14 (d, J_{CP} = 6 Hz), 124.73, 124.17, 123.64 (d, J_{CP} = 7 Hz), 123.25, 123.09, 122.79, 119.90, 119.45, 118.05, 117.81, 38.60, 35.36, 32.73 (d, J_{CP} = 7 Hz), 31.48. ^{31}P NMR ($CDCl_3$, 121 MHz,) δ (ppm): 264.91. HRMS (FTMS + p APCI, Toluene): 605.24393 m/z $[C_{39}H_{41}PS_2+H]^+$ (calcd for $C_{39}H_{41}PS_2$+H: 605.24655). Anal. Calcd for $C_{39}H_{41}PS_2$ (%): C, 77.45; H, 6.83. Found: C, 77.44; H, 6.85. UV/Vis/NIR (DCM): λ_{max} (ε) = 320 nm (22 400 $M^{-1}cm^{-1}$), 353 nm (26 700 $M^{-1}cm^{-1}$), 399 nm (shoulder, 5 300 $M^{-1}cm^{-1}$), 485 nm (900 $M^{-1}cm^{-1}$).

Attempted chemical polymerization of (2,7-bis(3-hexylthiophen-2-yl)-9H-fluoren-9-ylidene)(2,4,6-tri-tert-butylphenyl)phosphane and ^{31}P-NMR studies[1]:

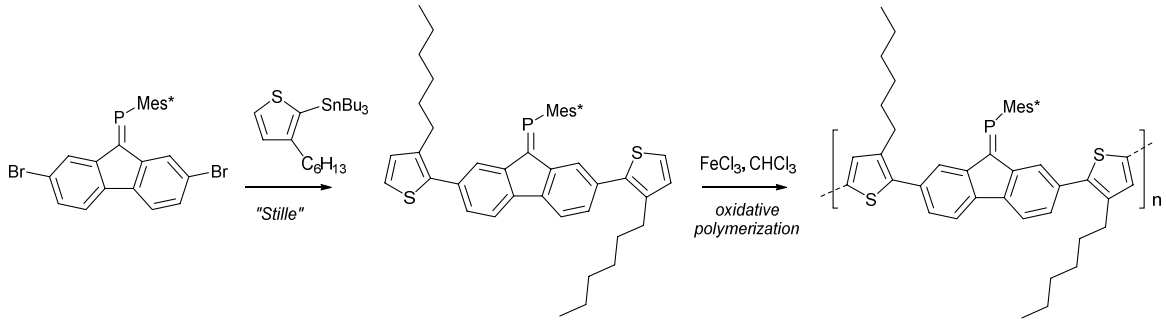

In order to prove a radical oxidative polymerization pathway through external positions leaving the double-bond intact, (2,7-bis(3-hexylthiophen-2-yl)-9H-fluoren-9-ylidene)(2,4,6-tri-tert-butylphenyl)phosphane was prepared analogously to **2a** from **1a** and 3-hexyl-2-(tributyl-stannyl)thiophene. The monomer has a typical ^{31}P NMR chemical shift of 268.20 ($CDCl_3$, 121 MHz). Then, in a flame-dried vial (2,7-bis(3-hexylthiophen-2-yl)-9H-fluoren-9-ylidene)(2,4,6-tri-tert-butylphenyl)phosphane (1 eq.) and iron trichloride (5 eq.) were stirred in chloroform for 48 hours; the reaction mixture turned purple, then hydrazine hydrate (~15 eq.) was added to the mixture, which

turned light-yellow-green. The crude organic mixture was washed with H_2O, extracted into chloroform and evaporated. Besides other unidentified species the broad ^{31}P NMR resonance 268.32 ppm ($CDCl_3$, 121 MHz,) is assigned to the corresponding polymer with intact phosphaalkene moieties. This proof-of-principle reaction supports a similar polymerization pathway during electropolymerization; over-oxidation by $FeCl_3$ and/or decomposition during the work-up naturally leads to other unidentified species.

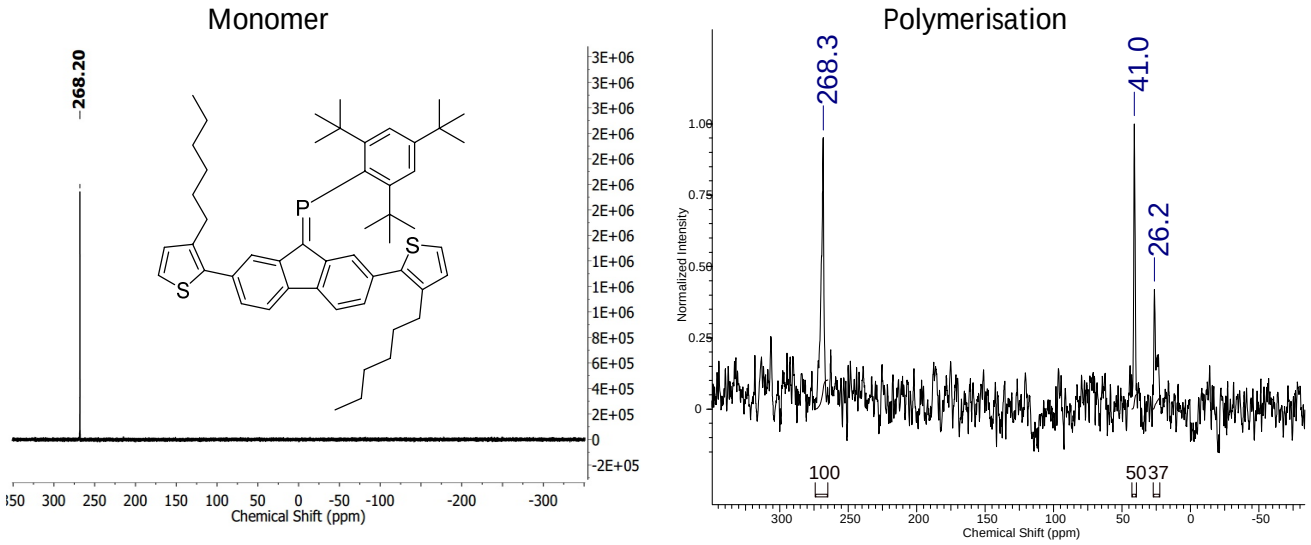

Synthesis of (2,7-dibromo-9H-fluoren-9-ylidene)(2,4,6-tri-tert-butylphenyl)arsane (**1b**):

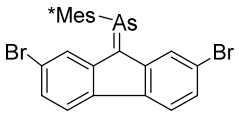

To a solution of 2-bromo-1,3,5-tri-tert-butylbenzene (3 g, 9.22 mmol) in 60 mL of THF at -78 °C, *n*-BuLi (3.69 mL, 9.22 mmol) was added dropwise. After 15 minutes, $AsCl_3$ (0.86 mL, 10.14 mmol) was added and the reaction was stirred at -78 °C. In a second flask, *n*-BuLi (3.87 mL, 9.68 mmol) was added to a solution of 2,7-dibromo-9H-fluorene (3.14 g, 9.68 mmol) in THF (60 mL) at -78 °C and after 30 minutes, the solution containing dichloro(2,4,6-tri-tert-butylphenyl)arsane was added using a cannula. After 30 minutes, DBU (1.45 mL, 9.68 mmol) was added to the reaction mixture at -78 °C, and the reaction mixture was left stirring overnight. The resulting dark orange solution was filtered through a plug of silica gel, concentrated under reduced pressure and purified by column chromatography (pentane, Rf: 0.4) to yield **1b** as an orange solid (4.92 g, 83% yield). ^1H NMR ($CDCl_3$, 400 MHz) δ (ppm): 8.38 (s, 1H), 7.64 (s, 2H), 7.43 (s, 2H), 7.36 (d, *J* = 8 Hz), 7.29 (dd, *J* = 8 Hz, 2.5 Hz, 2H), 5.60 (s, 1H), 1.45 (s, 9H), 1.41 (s, 18H). ^{13}C NMR ($CDCl_3$, 125 MHz) δ (ppm): 180.55, 154.64, 151.95, 145.63, 142.19, 136.41, 136.07, 134.54, 130.52, 130.32, 129.30, 123.52,

123.41, 121.02, 120.97, 120.22, 119.55, 36.83, 35.28, 33.11, 31.64. HRMS (FTMS + p APCI, toluene): 643.03711 m/z $[M+H]^+$ (calcd for $C_{31}H_{35}AsBr_2$+H: 643.03793). Anal. Calcd for $C_{31}H_{35}Br_2As$ (%): C, 57.97; H, 5.49. Found: C, 58.06; H, 5.62. UV/Vis/NIR (DCM): λ_{max} (ε) = 283 nm (22 600 $M^{-1}cm^{-1}$), 292 nm (25 900 $M^{-1}cm^{-1}$), 398 nm (11 600 $M^{-1}cm^{-1}$).Synthesis of (2,7-di(thiophen-2-yl)-9H-fluoren-9-ylidene)(2,4,6-tri-tert-butylphenyl)arsane (**2b**):

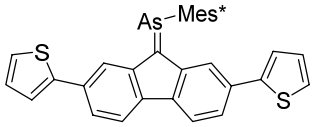

1b, (0.36 g, 0.56 mmol), 2-(tributylstannyl)thiophene (0.44 mL, 1.40 mmol), CsF (0.10 g, 0.67 mmol), $[PdCl_2(PPh_3)_2]$ (19.7 mg, 0.028 mmol) and THF (1.5 mL) were added to a dry microwave tube under argon. The solution was degassed thoroughly for 45 minutes, and the capped tube was placed in a microwave reactor (CEM, Biotage) at 120 °C for 15 minutes. The crude reaction mixture was filtered through a pad of silica, concentrated under reduced pressure and purified by column chromatography (90:10 pentane:DCM; R_f: 0.5) to yield **2b** as a dark reddish solid (80 mg, 40% yield). ^{1}H NMR ($CDCl_3$, 400 MHz) δ (ppm): 8.52 (s, 1H), 7.66 (s, 2H), 7.60 (m, 2H), 7.52 (d, *J* = 8 Hz, 2H), 7.45 (m, 2H), 7.31 (dd, *J* = 5.2 Hz, 1.2 Hz, 2H), 7.13 (m, 2H), 6.94 (m, 1H), 6.72 (dd, *J* = 5.2 Hz, 1.2 Hz, 1H), 6.60 (m, 1H), 1.47 (s, 18H), 1.40 (s, 9H). ^{13}C NMR ($CDCl_3$, 125 MHz) δ (ppm): 182.02, 154.84, 150.97, 145.11, 144.98, 144.97, 142.18, 137.55, 137.38, 135.49, 133.29, 132.77, 128.13, 128.04, 126.10, 125.77, 124.67, 124.08, 123.61, 123.39, 123.17, 122.60, 120.08, 119.44, 117.95, 38.89, 35.29, 32.96, 31.51. HRMS (FTMS + p NSI): 1329.37380 m/z [(2M+O) +H] (calcd for 2($C_{39}H_{41}AsS_2$+O)+H: 1329.37078). Anal. Calcd for $C_{39}H_{41}AsS_2$ (%): C, 72.20; H, 6.37. Found: C, 71.60; H, 6.60. UV/Vis/NIR (DCM): λ_{max} (ε) = 330 nm (35 800 $M^{-1}cm^{-1}$), 351 nm (31 600 $M^{-1}cm^{-1}$), 409 nm (12 400 $M^{-1}cm^{-1}$), 530 (1 300 $M^{-1}cm^{-1}$).

Synthesis of chlorido[(2,7-di(thiophen-2-yl)-9H-fluoren-9-ylidene)(2,4,6-tri-tert-butylphenyl)phosphane]gold(I) (**2a-AuCl**):

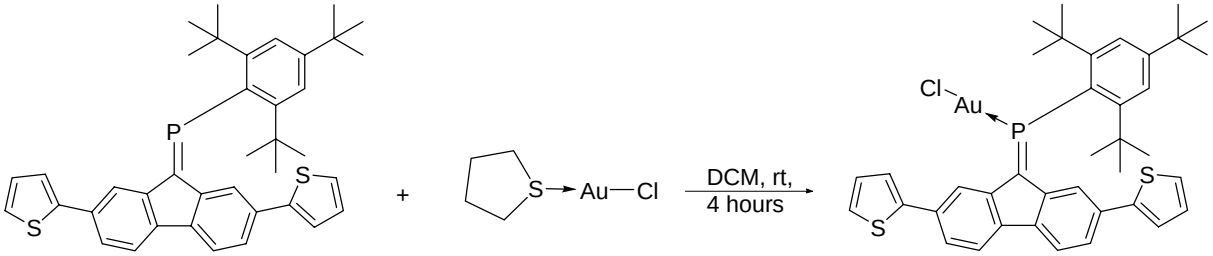

In a flame-dried microwave tube under argon, **2a** (1 eq.) was dissolved in DCM at room temperature, and purged with argon for 30 minutes. Then, chlorido(tetrahydrothiophene)gold(I) was added (1 eq.); the colour of the reaction mixture changed from red-violet to light green. Product formation (*quantitative*, ~15 mg) was monitored by ^{31}P NMR of the crude mixture using a filled capillary tube (d_6-benzene) as the solvent reference. Reaction completion was characterized by a change in the ^{31}P NMR chemical shift of the starting material from 264.9 ppm to 180.0 ppm. ^{1}H NMR ($CDCl_3$, 400 MHz) δ (ppm): 9.71 (d, *J* = 5.6 Hz, 1H), 7.80 (d, *J* = 3.6 Hz, 2H), 7.72 (ddd, *J* = 7.9, 3.1, 1.5 Hz, 1H), 7.62 – 7.45 (m, 4H), 7.33 (dd, *J* = 5.2, 1.2 Hz, 1H), 7.16 (m, 2H), 6.94 (dd, *J* = 5.1, 3.6 Hz, 1H), 6.73 (dd, *J* = 3.5, 1.1 Hz, 1H), 6.27 (d, *J* = 3.4 Hz, 1H), 1.64 (s, 18H), 1.40 (s, 9H). ^{13}C NMR ($CDCl_3$, 100 MHz) δ = 156.02 (d, J_{CP} = 9.6 Hz), 155.39 (d, J_{CP} = 11.2 Hz), 143.90, 143.41, 139.82 (d, J_{CP} = 53.6 Hz), 139.53 (d, J_{CP} = 21.6 Hz), 138.65 (d, J_{CP} = 70 Hz), 137.50 (d, J_{CP} =70 Hz), 134.58 (d, J_{CP} = 21.6 Hz), 134.24 (d, J_{CP} = 55 Hz), 133.45 (d, J_{CP} = 24 Hz), 132.06 (d, J_{CP} = 10.4 Hz), 129.38, 129.26, 128.64, 128.30 (dd, J_{CP} = 20 Hz, J_{CP} = 31 Hz), 128.11, 125.44, 125.31 (d, J_{CP} = 39.2 Hz), 124.77, 124.11, 123.42 (d, J_{CP} = 41.6 Hz), 122.92, 120.39, 119.33 (d, J_{CP} = 57.6 Hz), 39.60, 35.71, 34.23, 31.17. ^{31}P NMR ($CDCl_3$, 121 MHz,) δ (ppm): 180.03. HRMS (FTMS + p NSI, $CHCl_3$/CH_3CN): 859.16427 m/z $[C_{39}H_{41}AuClNaPS_2]^+$ (calcd for $C_{39}H_{41}AuClNaPS_2$: 859.16336), MALDI: m/z 836.24 $[M^+]$ (Calcd for $C_{39}H_{41}AuClPS_2$: 836.17). UV/Vis/NIR (DCM): λ_{max} (ε) = 333 nm, 356 nm (shoulder), 369 nm (shoulder), 402 (shoulder), 557 (centre of broad band).

a)

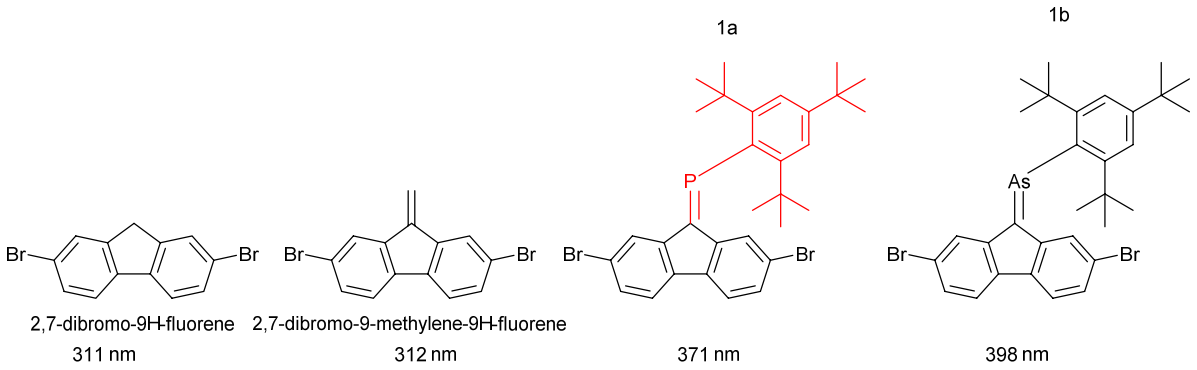

b)

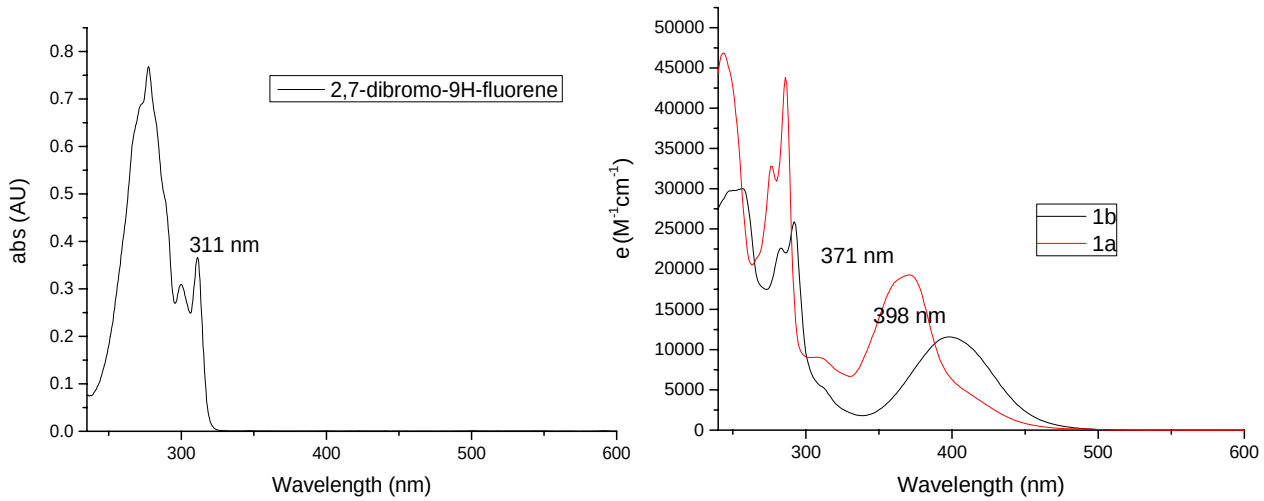

c)

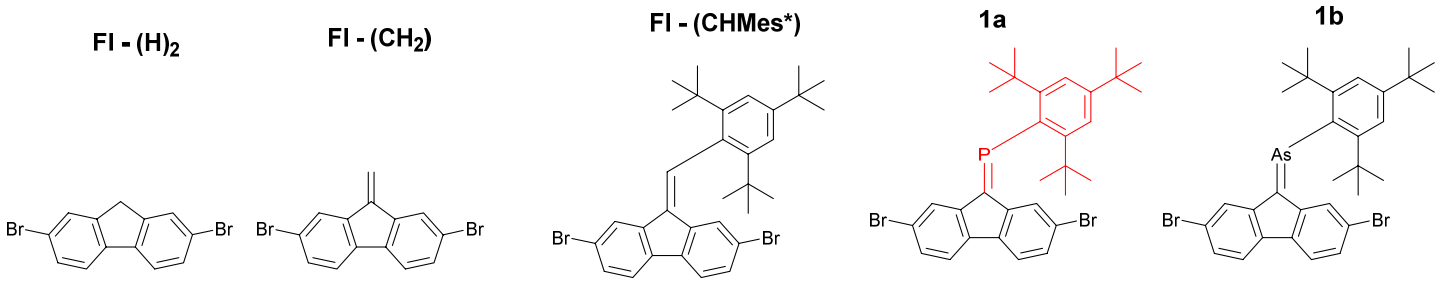

Species	Excited State # (nm)				
	1	**2**	**3**	**4**	**5**
Fl-(H)$_2$	287	278	232	226	226
Fl-(CH$_2$)	374	295	286	271	261
Fl–(CHMes*)	368	337	315	298	295
1a	469	433	372	371	318
1b	501	443	406	388	329

Figure S1. a) Comparison of molecular structures of parent compounds 2,7-dibromo-9H-fluorene, 2,7-dibromo-9-methylene-9H-fluorene[2], **1a**, and **1b;** wavelength of absorption maximum written below

b) Comparison of experimental UV-Vis spectra of 2,7-dibromo-9*H*-fluorene (left), **1a** and **1b** (right).

c) Comparison of molecular structures of parent compounds 2,7-dibromo-9H-fluorene, 2,7-dibromo-9-methylene-9H-fluorene, 2,7-dibromo-9-(2,4,6-tri-tert-butylbenzylidene)-9H-fluorene **1a**, and **1b**; table below structures displays five lowest energy transitions.

a)

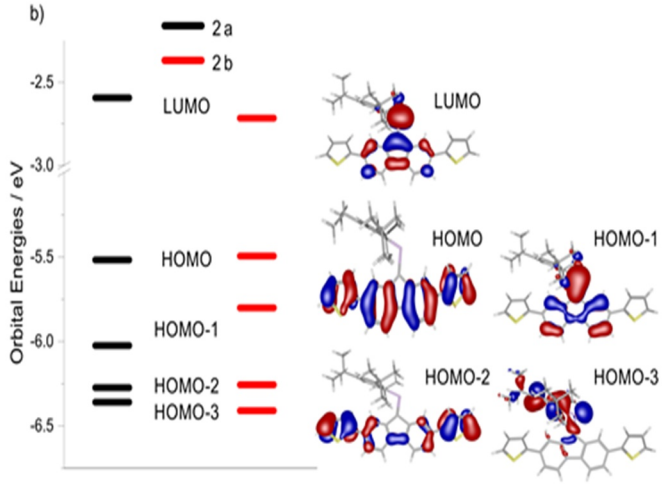

b)

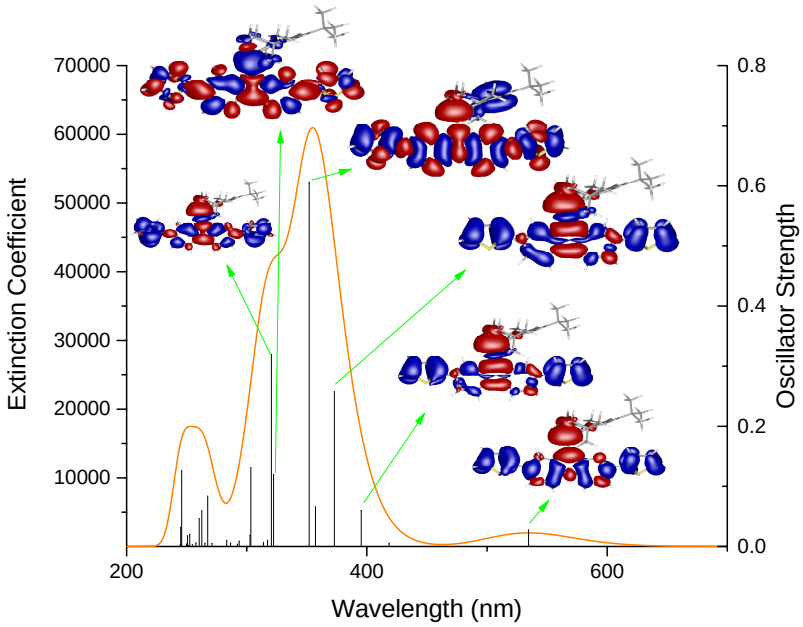

Wavelength (nm)	Oscillator Strength
535	0.0275
395	0.0601
373	0.2576
352	0.606
322	0.12
321	0.3194

c)

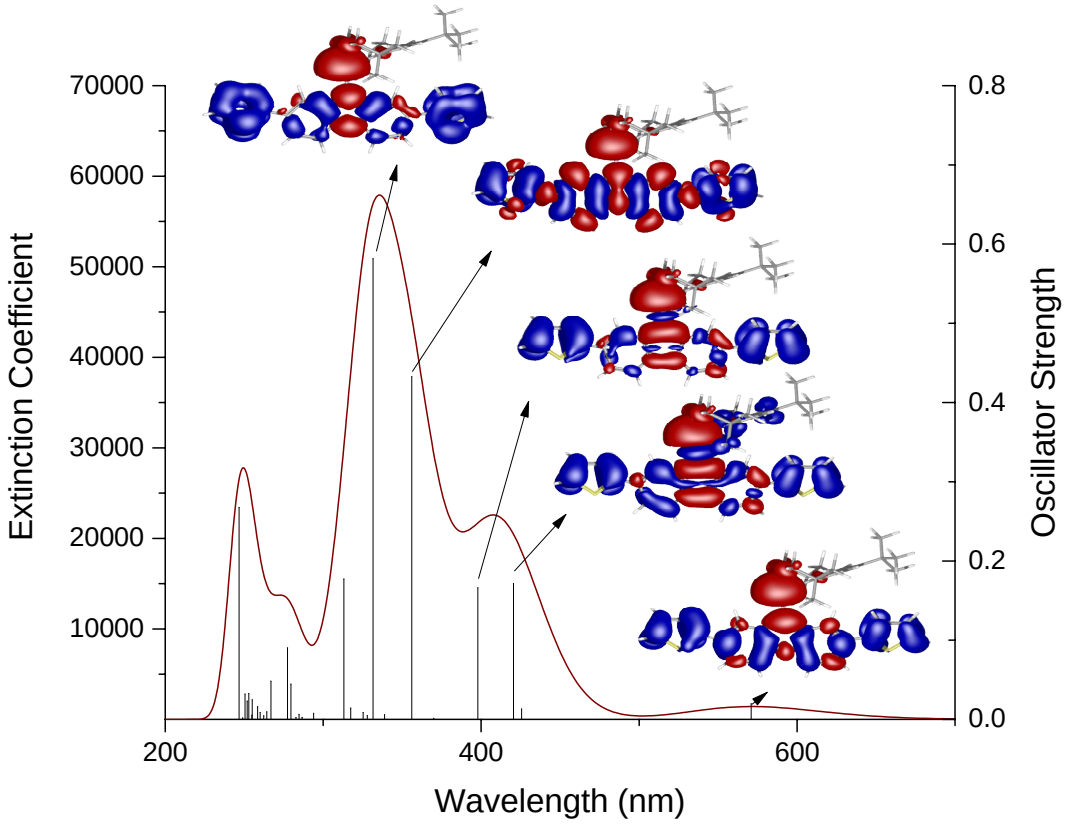

Figure S2. a) Frontier orbitals of 2a and 2b: HOMO-3 (lone pair to LUMO. Orbitals are only shown for 2b. b) c) Calculated UV-Vis spectra using a time-dependent hybrid functional (TD-B3LYP/6-311G**; gas phase); blue: decrease of electron density, red: increase of electron density b) **2a**, EDDM plots for selected electronic transitions; c) **2b**, EDDM plots for selected electronic transitions.

Wavelength (nm)	Oscillator Strength
571	0.0197
420	0.1716
398	0.1662
356	0.4326
332	0.5815

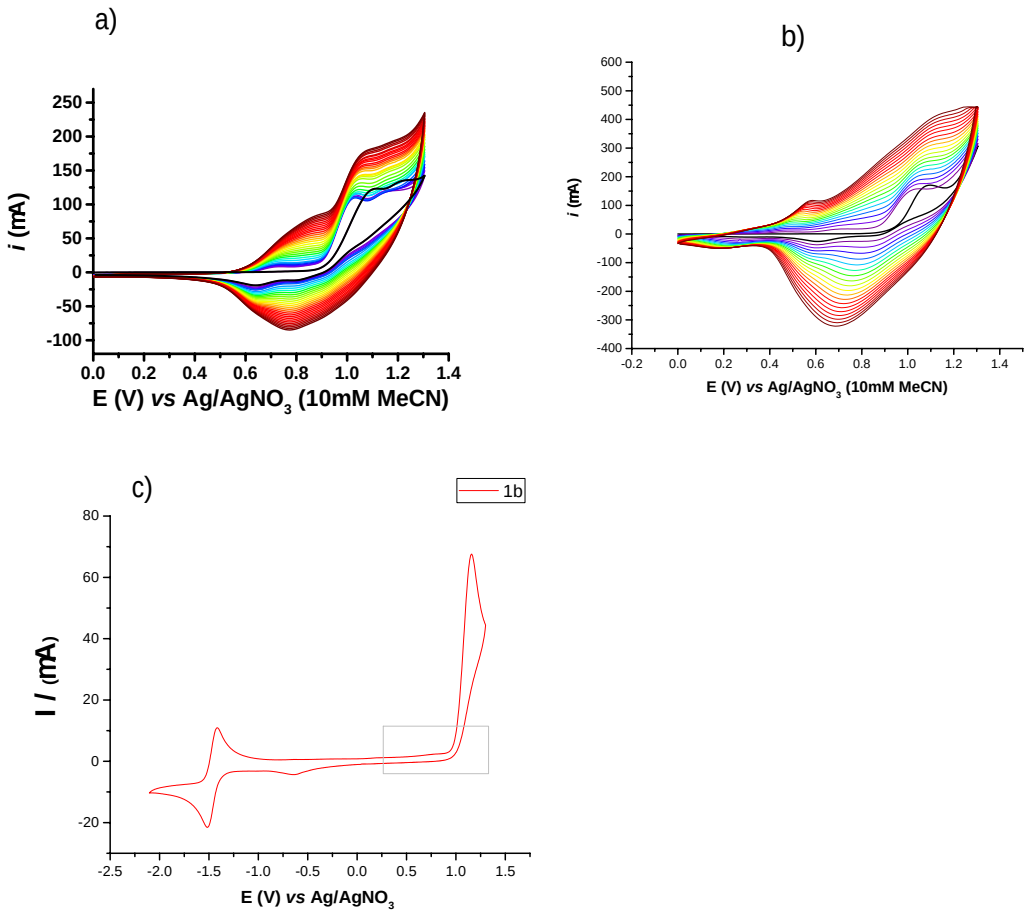

Figure S3. Selected electropolymerization voltammograms **a) 2a b) 2b** on FTO glass electrodes (1st to 20th scan) in a 0.1 mM *n*-Bu_4NPF_6 DCM solution at a scan rate of 100 mV s^{-1}, scan 1 black curve. **c)** Cyclic voltammogram of 1b (0 to 1.3 V), scan rate of 100 mV s^{-1}, following the irreversible oxidative peak, no potential-shifted current wave on the cathodic scan revealed no chemical process on the electrode surface had occurred (grey rectangle)

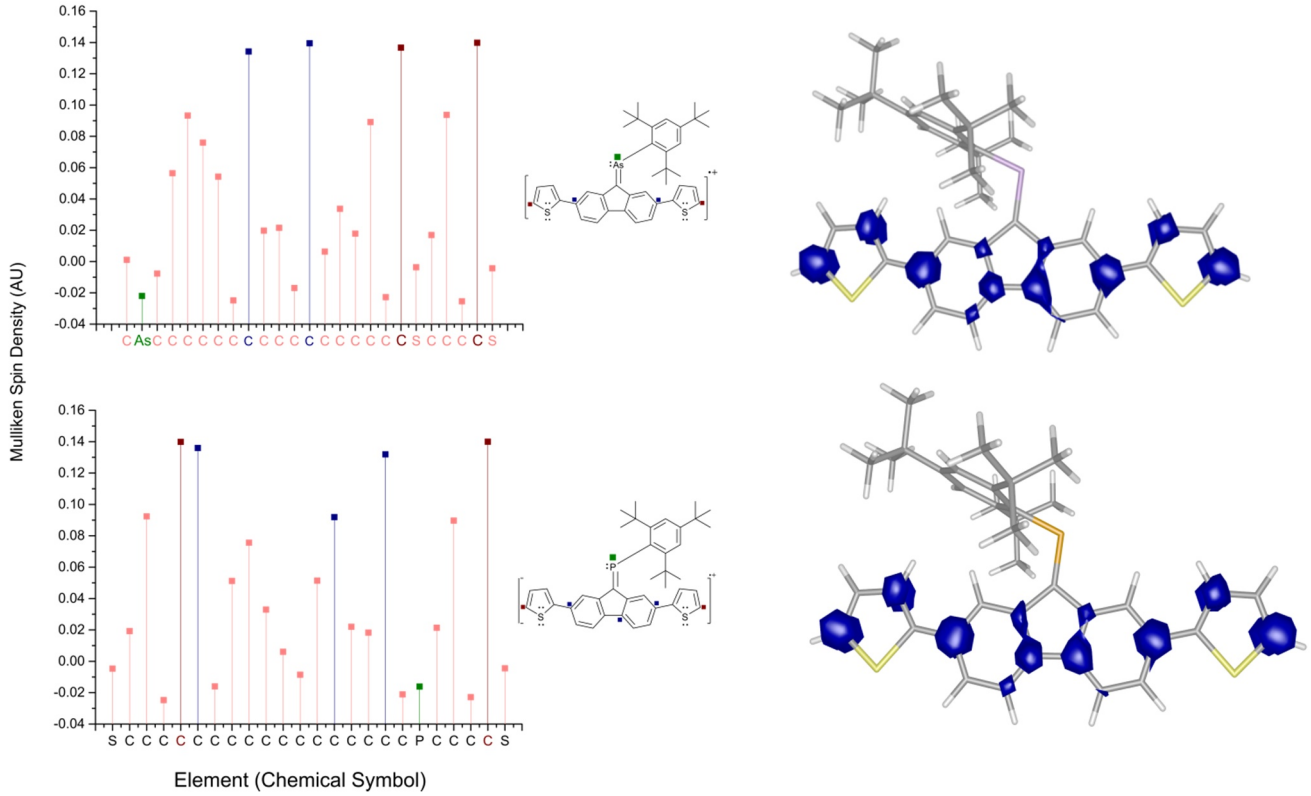

Figure S4. B3LYP/6-311G** optimized structures and calculated spin density of **2a**$^{\cdot+}$ (left) and **2b**$^{\cdot+}$ (right), rectangles show highest Mulliken Atomic Spin Density, which is located on the external α-carbons.

a) *2b* EDX analysis

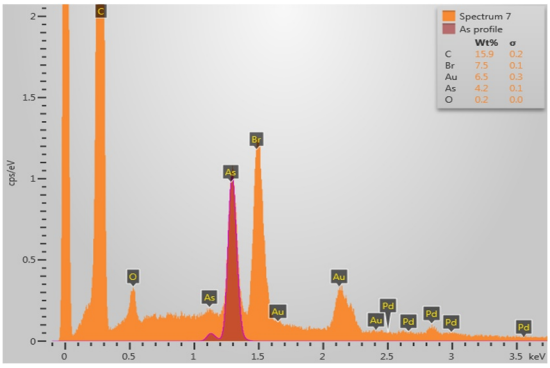

b) *poly-2a* EDX analysis

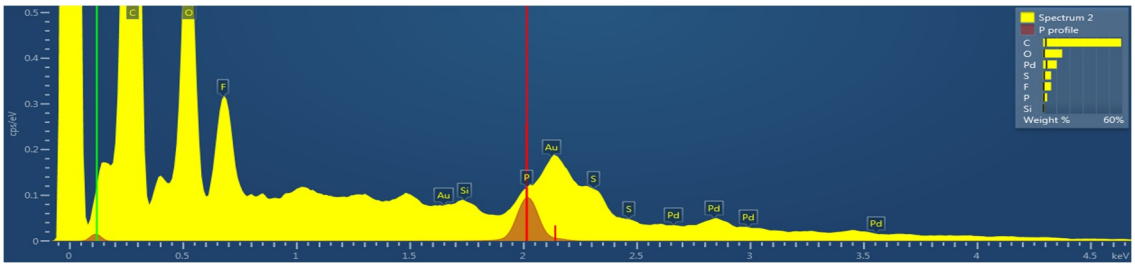

Weight % Spectrum Label	C	O	F	Si	P	S	Pd	Total	Project Path
Spectrum 1	75.08	13.72	4.81	0.55	**1.49**	**2.88**	1.47	100.00	sample4/Specimen 1/Site 1

c) *poly-2b* EDX analysis

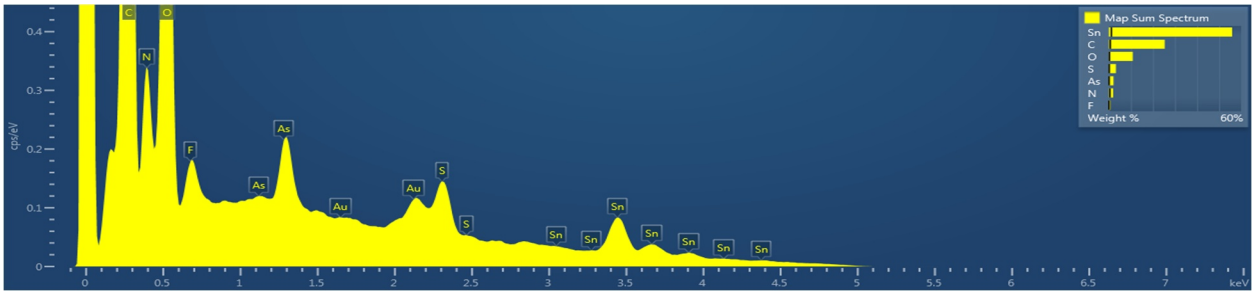

Weight % Spectrum Label	C	O	F	P	S	As	Pd	Total	Project Path
Spectrum 1	72.44	2.30	1.20	1.23	**10.98**	**6.39**	5.47	100.00	sample7/Specimen 2/Site 3

d) Spectrum 2 (FTO-substrate)

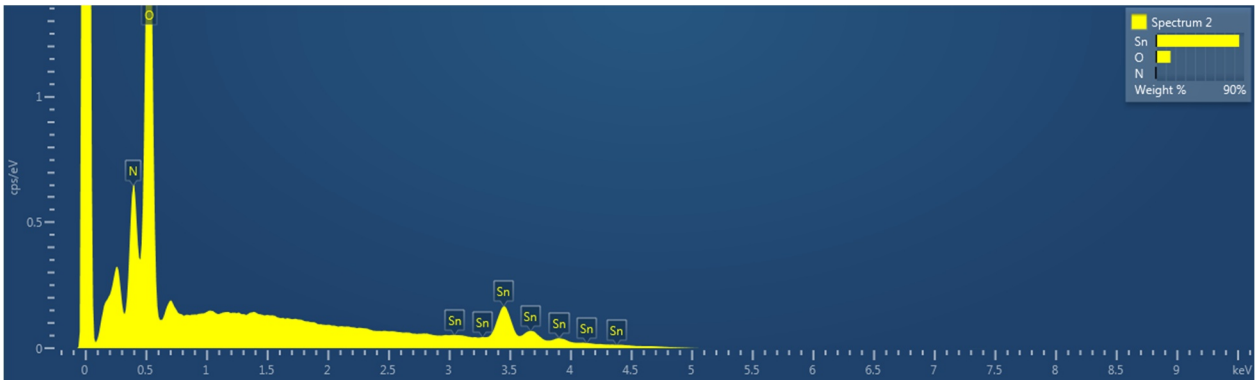

Figure S5. EDX spectra a) **2b** b) ***poly-2a*** c) ***poly-2b*** d) substrate films.

XPS Analysis/Discussion

XPS measurements were conducted using a Physical Electronics Quantum 2000 spectrometer (PHI Quantum 2000 Scanning ESCA), employing a monochromatic Al K_{α}-1486.6 eV X-ray beam and a photoelectron take-off angle of 45°. High resolution and survey spectra were acquired using 150, or 200 µm wide X-ray spots. An electron neutralizer was employed to compensate charging of the samples (20 µA, 1.20 V). All samples were quickly transferred into the instrument (chamber door: 9×10^{-7} bar, analysis chamber: 5×10^{-10} bar) to avoid moisture and air contamination after they were taken out from a glove box under Ar. In order to increase the energy resolution to two decimal units, the pass energy of the detector on the narrow scans (i.e. high-resolution spectra) was set at 29.35 eV; the wide-survey spectra were recorded at pass energy of 117.4 eV. For each sample, the corresponding parameters of two cycles, 100 steps per second and 20 sweeps were used. The fitting of the obtained spectra was performed with the software CasaXPS version 2.3.17.

As previously described, the monomers **(1a, 1b, 2a,** and **2b)** are indefinitely air stable in the solid state, and their phosphorus-carbon and arsenic-carbon double bond was characterized thoroughly. In spite of their stability, the compounds were transferred to an argon-filled glove box (<0.1 ppm O_2 and H_2O) and deposited on FTO glass substrates by drop-casting (DCM). The process yielded homogeneous films, which together with the polymers (***poly-2a*** and ***poly-2b)*** were transferred to the spectrometer room stored under argon. Therefore, the monomer samples were composed of phosphaalkene and arsaalkene moieties exclusively, and were used as an internal standard for the spectral characterization and analysis of ***poly-2a*** and ***poly-2b***.

Quantification/Survey Spectra

The quantification of the samples was done using the survey scan spectra. The choice of background on the different regions of the survey spectra did not significantly affect the atomic percentages, therefore, Tougaard and/or Shirley backgrounds were used during the quantification step (the same type of background was used within each sample analysis). Due to the relatively lower count rates in order not to cause x-ray damage, the quantitative analyses using survey spectra only provide a rough estimate of the relative atomic ratios. The spectra presented atomic % ratios close to 1:2 for P or As (Figure S8 and S9) with respect to Br (**1a**, **1b**) or S (**2a**, ***poly-2a***, **2b**, ***poly-2b***) atoms. Expectedly, carbon is the major species across all samples; contamination of oxygen and silicon (grease, monomers only) is also present, which is typical of the very surface (<10 nm) of the material. The survey spectra of ***poly-2a*** showed fluorine due to remaining electrolyte (NBu_4PF_6) from the polymerization procedure, and was reflected by the appearance of a phosphorus peak at higher BE on the P 2p narrow scan (see below).

Narrow scan Discussion

1a, 1b, 2a, 2b, *poly-2a*, *poly-2b*:

The raw C 1s spectra of all samples exhibit a relatively similar narrow peak at around 1.36 eV centred at around 283.51±0.10 eV before any charge correction was applied. The raw P 2p spectra present a major feature at lower BE (~129.5 eV), a second feature at around 132.5 eV, and a third one at a BE of around 136 eV (for ***poly*-2a** and ***poly*-2b**). The As 3d spectra present a major peak at around 41.5 eV, and a second overlapping feature at around 43.5 eV which is not close enough to arise from 3d spin-orbit splitting (ΔE=0.7 eV). The raw spectra serve to qualitatively compare the striking similarities between the monomer and polymer samples; also, due to the precision on the peak BE across all experiments (n=17), one concludes that charge correction of the sample surface by the electron neutralizer was successful.

In order to resolve the local chemical environment in the samples, the high-resolution spectra of C 1s, P 2p, S 2p, and As 3d were fitted with mixed Lorentzian/Gaussian product functions GL(%Lorentzian) using a Marquardt-Levenberg optimization algorithm, after subtracting a Shirley, Tougaard, or Linear background. After fittings were finished, the peak corresponding to sp^3 carbon atoms on the C 1s high-resolution spectra of all samples was referenced to carbon in a hydrocarbon environment of a polymer at 285.00 eV.[3] Experimentally, the fact that the peak on the high resolution spectra of C 1s is relatively symmetric, combined with its low BE at 283.5 eV (assuming an accurate absolute energy scale due to successful electron neutralization, as previously confirmed) indicates high non-oxidized sp^2 carbon contents. For the C 1s fitting, the area of the peaks was first constrained to be close to the expected stoichiometry, ($C_{31}Br_2E$, $C_{39}ES_2$). Three different carbon features were fitted to all spectra, corresponding to the sp^2 hybridized carbon atoms bonding to electronegative substituents (**1a**,**1b**: C-Br, ~6 at.% ; **2a**, **2b**, ***poly*-2a**, ***poly*-2b**: C-S, ~10 at.%), the sp^3 carbon atoms of the *tart*-butyl groups (**1a**,**1b**: ~39 at.%; **2a**, ***poly*-2a**, **2b**, ***poly*-2b**: ~31 at.%), and the rest (**1a**,**1b**: ~55 at.%; **2a**, ***poly*-2a**, **2b**, ***poly*-2b**: ~59 at.%). The used line-shape across all C 1s spectra was a GL(30). The full width at half maximum was kept from 0.9 to 1.3 eV, typical of carbon signals in organic compounds; additionally, the sp^2 hybrids were assigned the lowest BE, followed by the sp^3 atoms, with a separation of at least 0.5 eV between the two.[4] Similarly, the **C**-Br (**1a**, **1b**) and **C**-S subgroups were assigned a peak at higher BE than the sp^2 signal due to the higher oxidation state of its carbon atoms.[5] The π-π* shake-up satellite at a BE around 6 eV higher than the main sp^2 component overlapped with inelastically scattered electrons and was too weak compared to the noise, and since it is not a functional group it was excluded from the fitted data; however, its presence is evidence of conjugation across the systems.[6]

To account for spin-orbit splitting, the high-resolution spectra of P 2p, S 2p, and As 3d were fitted using doublets with an intensity ratio of 0.5, 0.51, and 0.67 for P, S, and As, respectively. Moreover, the energy separation within each doublet was 0.87 eV for P $2p_{3/2}$ and P $2p_{1/2}$, 1.16 eV for S $2p_{3/2}$ and S $2p_{1/2}$, and 0.7 eV for As $3d_{5/2}$ and As $3d_{3/2}$.[7] The FWHM varied from 1.03 to 1.45 eV for main signals, and the position of the BE was not constrained.

For all P 2p spectra, a Shirley background was subtracted. For **1a** and **2a** two components were fitted; the major peak at lower binding energies was assigned to phosphaalkenes, whereas the signal occurring around 3 eV at higher BE was assigned to pnictogen-containing impurities (e.g. oxidized impurities and/or X-ray damage, etc.)[8].

The FWHM of the peak assigned to oxidized phosphorus species was constrained to be less than 2.5 eV, as described in the literature, since the width of the photo-spectral lines for oxide impurities tends to be larger because of increased screening effects from phonon and local configuration interactions.[9] In addition to these two peaks, ***poly*-2a** samples displayed a third feature at higher BE (~136 eV which was assigned to phosphorus atoms from remaining NBu_4PF_6 supporting electrolyte used during the polymerization procedures, and agreeing well with previously described P 2p data.[8] This hypothesis was confirmed by comparing fresh samples of ***poly*-2a** to air-exposed ones for several hours, which led to an increase of the doublets at 132.79±0.07 eV, whereas the relative intensity of the signal at 135.94±0.13 eV (NBu_4PF_6 electrolyte) stayed stable (Figure S6c). Additionally and very importantly, in order to obtain satisfactory residuals, the C 1s of these samples (Figure S6, XI-IX) had to be fitted with an extra component at around 286.89±0.3 eV, which agrees with literature values for single-bonded carbon to oxygen.[10]

The analysis of the As 3d high-resolution spectra was performed analogously. For all As 3d spectra, two set of doublets were fitted. The signal at lower BE (see Figure S9) is present across all monomer and polymer samples, and was assigned to arsaalkene species. The peak at higher BE was assigned to oxidized impurities and/or defects, similarly as for high-resolution spectra of P 2p electrons.

Once the energy of the peaks was internally corrected across all samples (i.e. the sp^3 carbon signal was shifted to 285.00 eV, and all high-resolution spectra were shifted correspondingly), the BE of the assigned phosphaalkenes and arsaalkenes was studied (Table S1). Moreover, the data parameters and constraints used in the fitting process are shown in Table S2 (**1a**, **2a**, ***poly*-2a**) and Table S3 (**1b**, **2b**, ***poly*-2b**).

The quality of the fits was inspected through the residual curve after fitting, and by using extremely similar fits (i.e. constrained position, and FWHM) across different samples. The fitting parameters

were optimized in order to minimize the residual standard deviation (Residual STD) between the fitted and experimental spectra.[11] Values lower than 2 indicate the synthesized peak fits mathematically resembles the data envelope. Each fitting process was finished when the Residual STD changed by less than 0.05 units. Low Residual Standard Deviations (0.7-1.8) were obtained for all peak fits. The stability of the fittings across all samples, the qualitative features and reproducibility of the experimental data, combined with the well-known chemical characterization of the monomer samples before-hand, and most importantly, the small standard deviations obtained for the signals assigned to phosphaalkene at 129.98±0.08 and arsaalkene at 42.29±0.05, indicate the characterization of polymer films containing P=C and As=C double bonds.

Sample id	C (sp2)	P (P=C)	Sample id	C (sp^2)	As (As=C)
I (1a)	284.48	129.91	**I (1b)**	284.50	42.34
II (1a)	284.52	130.11	**II (1b)**	284.53	42.35
III (2a)	284.47	130.03	**III (2b)**	284.47	42.23
IV (2a)	284.48	130.05	**IV (2b)**	284.49	42.27
V (*poly*-2a)	284.43	130.01	**V (*poly*-2b)**	284.45	42.26
VI (*poly*-2a)	284.38	129.89	**VI (*poly*-2b)**	284.47	42.30
VII (*poly*-2a)	284.42	129.95	**VII (*poly*-2b)**	284.44	42.25
VIII (*poly*-2a)	284.43	129.93	**VIII (*poly*-2b)**	284.44	42.31
IX (*poly*-2a)	284.38	129.91			
Average	284.44	129.98	**Average**	284.474	42.29
Standard Deviation	0.05	0.08	**Standard Deviation**	0.030	0.05

Table S1. Analysis of assigned sp^2 hybridized carbon on C 1s, phosphaalkenes on P 2p, and arsaalkenes on As 3d high-resolution spectra across all samples.

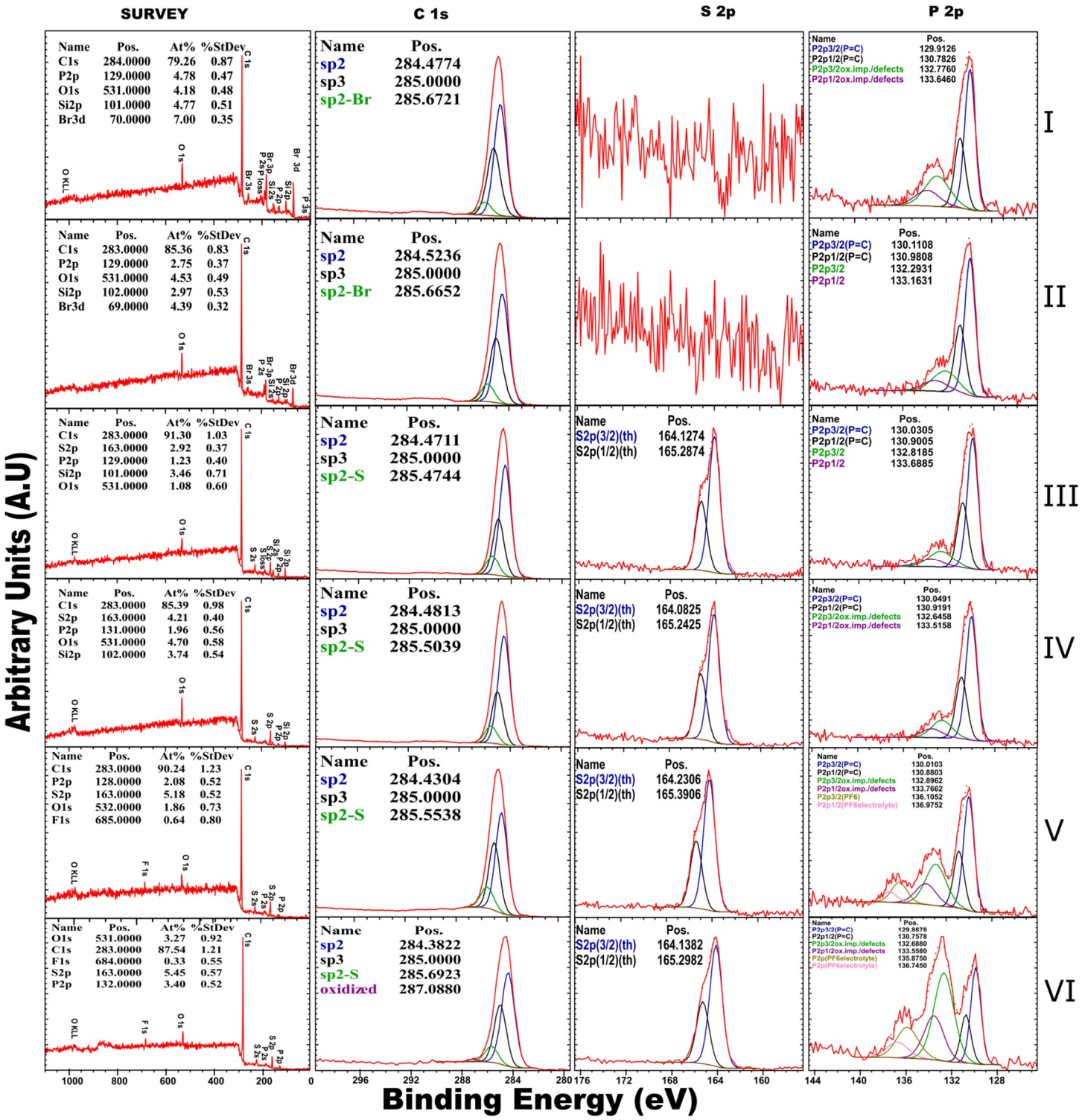

Continued on next page à

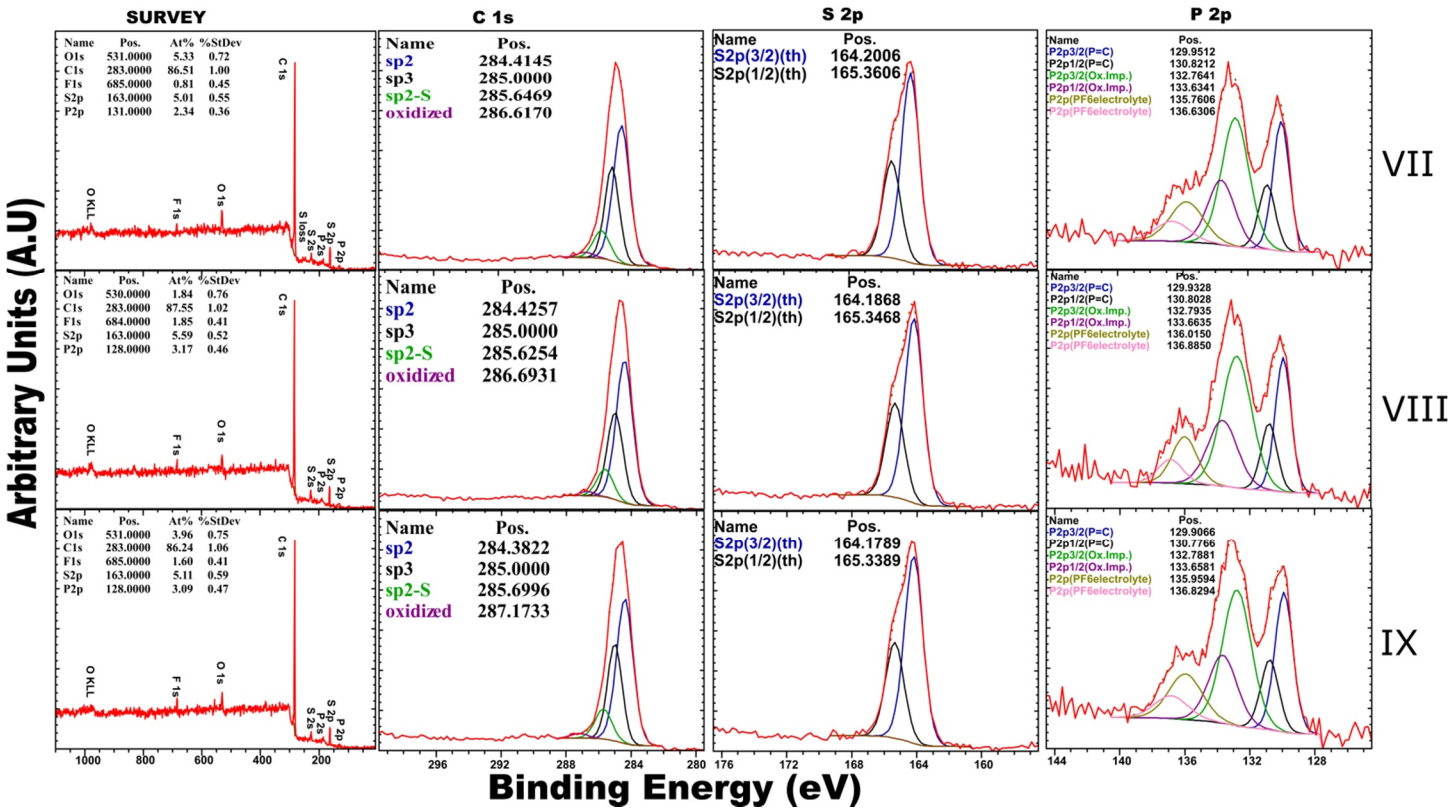

b)

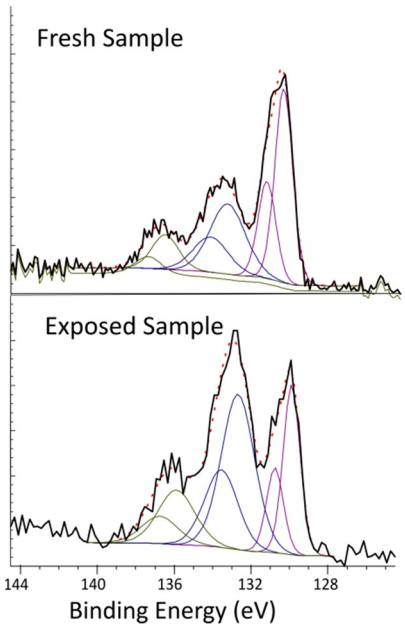

Figure S6. a) Survey and C 1s, S 2p, and P 2p high-resolution spectra of **1a (**I, II**), 2a (**III, IV**)**, and ***poly-2a (***V-IX***)*** samples **b)** Comparison of fresh vs. air-exposed for several hours samples of ***poly-2a***

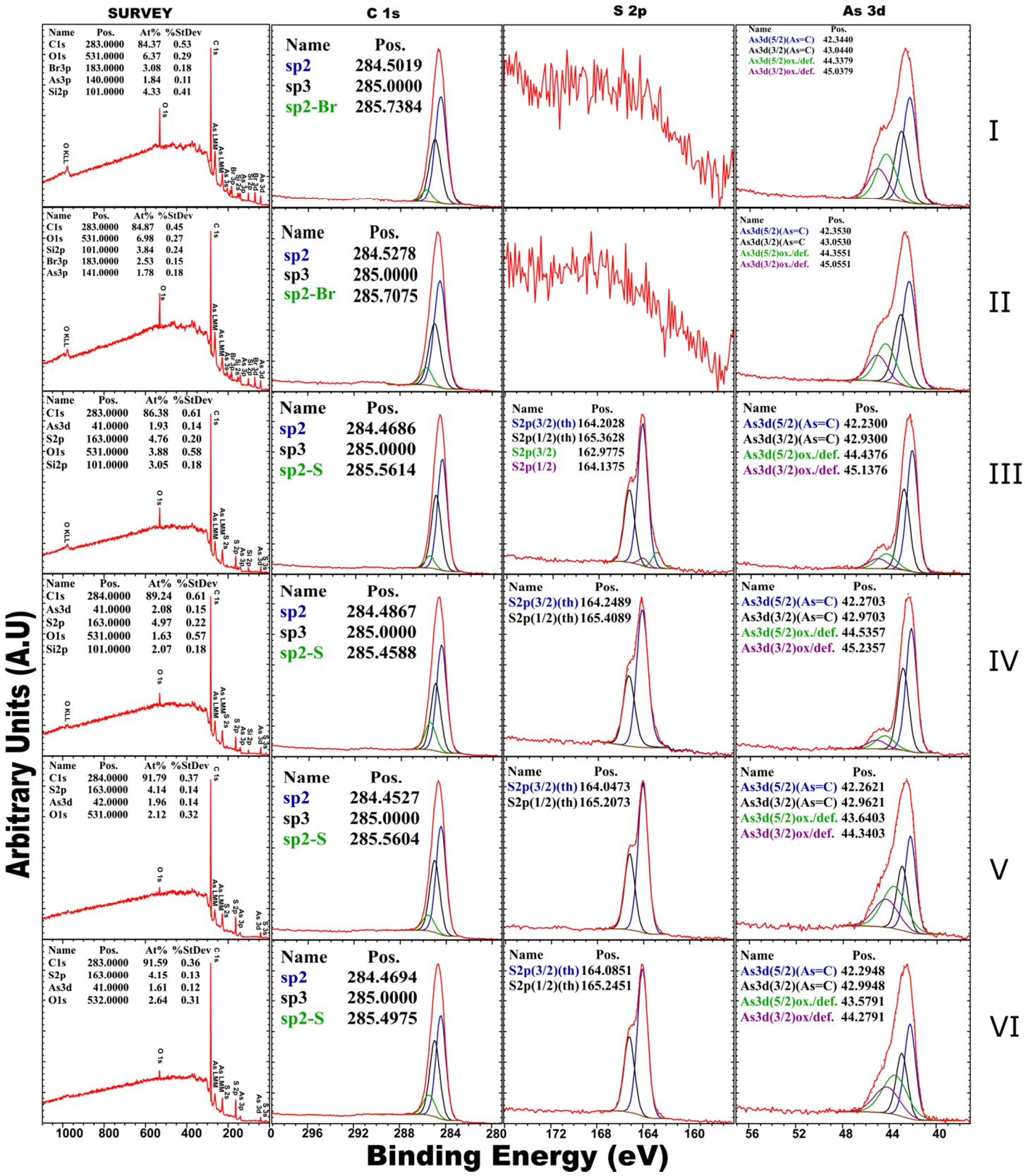

Continued on next page à

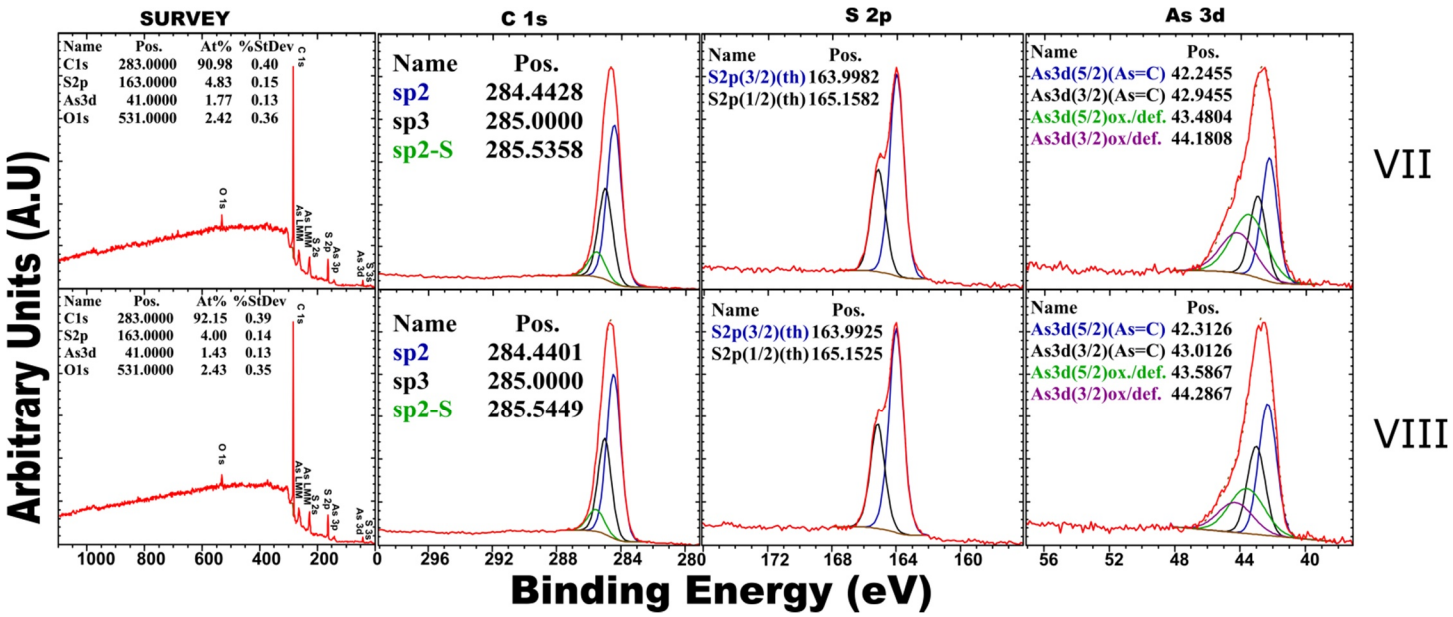

Figure S7. Survey and high-resolution C 1s, S 2p, and As 3d spectra of all **1b (I, II), 2b (III, IV)**, and ***poly*-2b *(V-VIII)*** samples. Red curve: Experimental Data, Dotted brown curve: Total Fitted Curve

C 1s

	Name	Pos.	FWHM	L.Sh.	Area	%Area	Pos Const	FWHM Const	Area Const	Const Id.
I	sp2	284.4774	1.1179	GL(30)	3008.51	56.35	284.5 , 283.5	0.9 , 1.2	0.0 , 10000.0	A
	sp3	285.0000	1.1957	GL(30)	1955.45	36.62	286 , 284.5	0.9 , 1.2	0.0 , 10000.0	B
	sp2-Br	285.6721	1.2000	GL(30)	375.85	7.04	287 , 284.5	0.9 , 1.2	0.0 , 2000.0	C
II	sp2	284.5236	1.1832	GL(30)	2921.68	56.85	284.529 , 283.529	0.5 , 1.5	0.0 , 10000.0	A
	sp3	285.0000	1.2000	GL(30)	1741.20	33.87	286 , 284.5	0.9 , 1.2	0.0 , 10000.0	B
	sp2-Br	285.6652	1.2000	GL(30)	476.94	9.28	287 , 284.5	0.9 , 1.2	0.0 , 2000.0	C
III	sp2	284.4711	1.0324	GL(30)	2846.14	59.38	285.5 , 283.5	0.9 , 1.25	0.0 , 10000.0	A
	sp3	285.0000	1.0166	GL(30)	1431.92	29.87	286 , 284.5	0.9 , 1.2	0.0 , 10000.0	B
	sp2-S	285.4744	1.1041	GL(30)	515.02	10.74	287 , 284.5	0.9 , 1.2	0.0 , 2000.0	C
IV	sp2	284.4813	1.0782	GL(30)	2830.69	61.78	285.5 , 283.5	0.9 , 1.25	0.0 , 10000.0	A
	sp3	285.0000	1.0258	GL(30)	1284.30	28.03	286 , 284.5	0.9 , 1.2	0.0 , 10000.0	B
	sp2-S	285.5039	1.1319	GL(30)	467.04	10.19	287 , 284.5	0.9 , 1.2	0.0 , 2000.0	C
V	sp2	284.4304	1.0885	GL(30)	2326.73	53.77	284.546 , 284.046	0.9 , 1.25	0.0 , 10000.0	A
	sp3	285.0000	1.0159	GL(30)	1464.69	33.84	286.001 , 284.501	0.9 , 1.2	0.0 , 10000.0	B
	sp2-S	285.5538	1.2000	GL(30)	536.17	12.39	287.001 , 284.501	0.9 , 1.2	0.0 , 2000.0	C
VI	sp2	284.3822	1.2000	GL(30)	3547.30	56.54	284.5 , 283.5	0.5 , 1.2	0.0 , 10000.0	A
	sp3	285.0000	1.1015	GL(30)	2058.66	32.81	286 , 284.5	0.9 , 1.22	2000.0 , 2250.0	B
	sp2-S	285.6923	1.2000	GL(30)	599.73	9.56	287 , 284.5	0.9 , 1.2	0.0 , 2000.0	C
	oxidized	287.0880	0.9247	GL(30)	68.89	1.10	289 , 286	0.2329 , 1.2	0.0 , 150.0	D
VII	sp2	284.4145	1.2000	GL(30)	3413.97	54.78	284.501 , 283.501	0.5 , 1.2	0.0 , 10000.0	A
	sp3	285.0000	1.0407	GL(30)	2011.42	32.22	286.001 , 284.501	0.9 , 1.22	0.0 , 10000.0	B
	sp2-S	285.6469	1.2000	GL(30)	684.55	10.97	287.001 , 284.501	0.9 , 1.2	0.0 , 2000.0	C
	oxidized	286.6170	1.2000	GL(30)	131.77	2.11	289.001 , 286.001	0.2256 , 1.2	0.0 , 150.0	D
VIII	sp2	284.4257	1.2000	GL(30)	3489.74	55.98	284.426 , 284.426	0.5 , 1.2	0.0 , 10000.0	A
	sp3	285.0000	1.1245	GL(30)	2000.18	32.08	286.001 , 284.501	0.9 , 1.22	0.0 , 10000.0	B
	sp2-S	285.6254	1.1536	GL(30)	653.79	10.48	287.001 , 284.501	0.9 , 1.2	0.0 , 2000.0	C
	oxidized	286.6931	1.0242	GL(30)	90.85	1.46	289.001 , 286.001	0.2339 , 5.846	0.0 , 150.0	D
IX	sp2	284.3822	1.2000	GL(30)	3462.65	54.91	284.5 , 283.5	0.5 , 1.2	0.0 , 10000.0	A
	sp3	285.0000	1.0398	GL(30)	2022.37	32.07	286 , 284.5	0.9 , 1.22	0.0 , 10000.0	B
	sp2-S	285.6996	1.2000	GL(30)	715.44	11.34	287 , 284.5	0.9 , 1.2	0.0 , 2000.0	C
	oxidized	287.1733	1.2000	GL(30)	106.63	1.68	289 , 286	0.2286 , 1.2	0.0 , 150.0	D

P 2p

	Name	Pos.	FWHM	L.Sh.	Area	%Area	Pos Const	FWHM Const	Area Const	Const Id.
I	P2p3/2(P=C)	129.9126	1.1000	GL(30)	103.92	44.40	132 , 128	1.1 , 1.4	0.0 , 10000000.0	A
	P2p1/2(P=C)	130.7826	1.1000	GL(30)	51.96	22.20	A + 0.87	A^1	A^0.5	B
	P2p3/2ox.imp./defects	132.7760	2.5000	GL(30)	52.16	22.27	136 , 129	0.7 , 2.5	0.0 , 100.0	C
	P2p1/2ox.imp./defects	133.6460	2.5000	GL(30)	26.08	11.13	C + 0.87	C^1	C^0.5	D
II	P2p3/2(P=C)	130.1108	1.1084	GL(30)	110.17	49.36	132 , 128	0.7 , 1.2	0.0 , 10000000.0	A
	P2p1/2(P=C)	130.9808	1.1084	GL(30)	55.08	24.68	A + 0.87	A^1	A^0.5	B
	P2p3/2	132.2931	2.5000	GL(30)	38.65	17.31	136 , 129	0.7 , 2.5	0.0 , 100.0	C
	P2p1/2	133.1631	2.5000	GL(30)	19.32	8.65	C + 0.87	C^1	C^0.5	D
III	P2p3/2(P=C)	130.0305	1.0954	GL(30)	79.23	52.48	132 , 128	0.7 , 1.3	0.0 , 10000000.0	A
	P2p1/2(P=C)	130.9005	1.0954	GL(30)	39.61	26.24	A + 0.87	A^1	A^0.5	B
	P2p3/2	132.8185	2.4318	GL(30)	21.44	14.19	136 , 129	0.7 , 2.5	0.0 , 100.0	C
	P2p1/2	133.6885	2.4318	GL(30)	10.72	7.09	C + 0.87	C^1	C^0.5	D
IV	P2p3/2(P=C)	130.0491	1.1338	GL(30)	70.46	52.83	132 , 128	0.7 , 1.3	0.0 , 10000000.0	A
	P2p1/2(P=C)	130.9191	1.1338	GL(30)	35.23	26.41	A + 0.87	A^1	A^0.5	B
	P2p3/2ox.imp./defects	132.6458	2.0809	GL(30)	18.47	13.84	136 , 129	0.7 , 2.5	0.0 , 100.0	C
	P2p1/2ox.imp./defects	133.5158	2.0809	GL(30)	9.24	6.92	C + 0.87	C^1	C^0.5	D
V	P2p3/2(P=C)	130.0103	1.0746	GL(30)	48.21	33.65	132.001 , 128.001	0.7 , 1.3	0.0 , 10000000.0	A
	P2p1/2(P=C)	130.8803	1.0746	GL(30)	24.10	16.82	A + 0.87	A^1	A^0.5	B
	P2p3/2ox.imp./defects	132.8962	2.1339	GL(30)	34.61	24.14	136.001 , 129.001	0.7 , 2.5	0.0 , 1000.0	C
	P2p1/2ox.imp./defects	133.7662	2.1339	GL(30)	17.30	12.07	C + 0.87	C^1	C^0.5	D
	P2p3/2(PF6)	136.1052	1.5978	GL(30)	12.73	8.88	140.001 , 134.001	0.7 , 2.5	0.0 , 1000.0	E
	P2p1/2(PFselectrolyte)	136.9752	1.5978	GL(30)	6.37	4.44	E + 0.87	E^1	E^0.5	F
VI	P2p3/2(P=C)	129.8878	1.0399	GL(30)	57.23	19.22	131.523 , 129.523	0.7 , 1.5	0.0 , 10000000.0	A
	P2p1/2(P=C)	130.7578	1.0399	GL(30)	28.61	9.61	A + 0.87	A^1	A^0.5	B
	P2p3/2ox.imp./defects	132.6880	2.0286	GL(30)	101.94	34.21	144.523 , 124.523	0.7 , 2.5	0.0 , 500.0	C
	P2p1/2ox.imp./defects	133.5580	2.0286	GL(30)	50.97	17.10	C + 0.87	C^1	C^0.5	D
	P2p(PFSelectrolyte)	135.8750	2.2374	GL(30)	39.47	13.24	144.523 , 124.523	0.7 , 2.5	0.0 , 10000000.0	E
	P2p(PFSelectrolyte)	136.7450	2.2374	GL(30)	19.73	6.62	E + 0.87	E^1	E^0.5	F
VII	P2p3/2(P=C)	129.9512	1.1983	GL(30)	59.33	20.47	131.393 , 129.393	0.7 , 1.5	0.0 , 10000000.0	A
	P2p1/2(P=C)	130.8212	1.1983	GL(30)	29.67	10.23	A + 0.87	A^1	A^0.5	B
	P2p3/2(Ox.Imp.)	132.7641	1.9679	GL(30)	96.86	33.40	144.393 , 124.393	0.7 , 2.5	0.0 , 500.0	C
	P2p1/2(Ox.Imp.)	133.6341	1.9679	GL(30)	48.43	16.70	C + 0.87	C^1	C^0.5	D
	P2p(PFSelectrolyte)	135.7906	2.4157	GL(30)	37.17	12.81	144.393 , 124.393	0.7 , 2.5	0.0 , 10000000.0	E
	P2p(PFSelectrolyte)	136.6306	2.4157	GL(30)	18.58	6.40	E + 0.87	E^1	E^0.5	F
VIII	P2p3/2(P=C)	129.9328	1.1539	GL(30)	57.56	19.71	131.543 , 129.543	0.7 , 1.5	0.0 , 10000000.0	A
	P2p1/2(P=C)	130.8028	1.1539	GL(30)	28.78	9.85	A + 0.87	A^1	A^0.5	B
	P2p3/2(Ox.Imp.)	132.7935	2.1645	GL(30)	105.85	36.23	144.543 , 124.543	0.7 , 2.5	0.0 , 500.0	C
	P2p1/2(Ox.Imp.)	133.6635	2.1645	GL(30)	52.93	18.11	C + 0.87	C^1	C^0.5	D
	P2p(PFSelectrolyte)	136.0150	1.7885	GL(30)	31.35	10.72	144.543 , 124.543	0.7 , 2.5	0.0 , 10000000.0	E
	P2p(PFSelectrolyte)	136.8850	1.7885	GL(30)	15.67	5.36	E + 0.87	E^1	E^0.5	F
IX	P2p3/2(P=C)	129.9066	1.2994	GL(30)	66.02	21.15	131.525 , 129.525	0.7 , 1.5	0.0 , 10000000.0	A
	P2p1/2(P=C)	130.7766	1.2994	GL(30)	33.01	10.57	A + 0.87	A^1	A^0.5	B
	P2p3/2(Ox.Imp.)	132.7881	2.0742	GL(30)	102.21	32.73	144.525 , 124.525	0.7 , 2.5	0.0 , 500.0	C
	P2p1/2(Ox.Imp.)	133.6581	2.0742	GL(30)	51.11	16.36	C + 0.87	C^1	C^0.5	D
	P2p(PFSelectrolyte)	135.9594	2.4134	GL(30)	39.98	12.79	144.525 , 124.525	0.7 , 2.5	0.0 , 10000000.0	E
	P2p(PFSelectrolyte)	136.8294	2.4134	GL(30)	19.99	6.40	E + 0.87	E^1	E^0.5	F

S 2p

	Name	Pos.	FWHM	L.Sh.	Area	%Area	Pos Const	FWHM Const	Area Const	Const Id.
III	P2p3/2(P=C)	130.0305	1.0954	GL(30)	79.23	52.48	132 , 128	0.7 , 1.3	0.0 , 10000000.0	A
	P2p1/2(P=C)	130.9005	1.0954	GL(30)	39.61	26.24	A + 0.87	A^1	A^0.5	B
	P2p3/2	132.8185	2.4318	GL(30)	21.44	14.19	136 , 129	0.7 , 2.5	0.0 , 100.0	C
	P2p1/2	133.6885	2.4318	GL(30)	10.72	7.09	C + 0.87	C^1	C^0.5	D
IV	P2p3/2(P=C)	130.0491	1.1338	GL(30)	70.46	52.83	132 , 128	0.7 , 1.3	0.0 , 10000000.0	A
	P2p1/2(P=C)	130.9191	1.1338	GL(30)	35.23	26.41	A + 0.87	A^1	A^0.5	B
	P2p3/2ox.imp./defects	132.6458	2.0809	GL(30)	18.47	13.84	136 , 129	0.7 , 2.5	0.0 , 100.0	C
	P2p1/2ox.imp./defects	133.5158	2.0809	GL(30)	9.24	6.92	C + 0.87	C^1	C^0.5	D
V	P2p3/2(P=C)	130.0103	1.0746	GL(30)	48.21	33.65	132.001 , 128.001	0.7 , 1.3	0.0 , 10000000.0	A
	P2p1/2(P=C)	130.8803	1.0746	GL(30)	24.10	16.82	A + 0.87	A^1	A^0.5	B
	P2p3/2ox.imp./defects	132.8962	2.1339	GL(30)	34.61	24.14	136.001 , 129.001	0.7 , 2.5	0.0 , 1000.0	C
	P2p1/2ox.imp./defects	133.7662	2.1339	GL(30)	17.30	12.07	C + 0.87	C^1	C^0.5	D
	P2p3/2(PF6)	136.1052	1.5978	GL(30)	12.73	8.88	140.001 , 134.001	0.7 , 2.5	0.0 , 1000.0	E
	P2p1/2(PFselectrolyte)	136.9752	1.5978	GL(30)	6.37	4.44	E + 0.87	E^1	E^0.5	F
VI	P2p3/2(P=C)	129.8878	1.0399	GL(30)	57.23	19.22	131.523 , 129.523	0.7 , 1.5	0.0 , 10000000.0	A
	P2p1/2(P=C)	130.7578	1.0399	GL(30)	28.61	9.61	A + 0.87	A^1	A^0.5	B
	P2p3/2ox.imp./defects	132.6880	2.0286	GL(30)	101.94	34.21	144.523 , 124.523	0.7 , 2.5	0.0 , 500.0	C
	P2p1/2ox.imp./defects	133.5580	2.0286	GL(30)	50.97	17.10	C + 0.87	C^1	C^0.5	D
	P2p(PFSelectrolyte)	135.8750	2.2374	GL(30)	39.47	13.24	144.523 , 124.523	0.7 , 2.5	0.0 , 10000000.0	E
	P2p(PFSelectrolyte)	136.7450	2.2374	GL(30)	19.73	6.62	E + 0.87	E^1	E^0.5	F
VII	P2p3/2(P=C)	129.9512	1.1983	GL(30)	59.33	20.47	131.393 , 129.393	0.7 , 1.5	0.0 , 10000000.0	A
	P2p1/2(P=C)	130.8212	1.1983	GL(30)	29.67	10.23	A + 0.87	A^1	A^0.5	B
	P2p3/2(Ox.Imp.)	132.7641	1.9679	GL(30)	96.86	33.40	144.393 , 124.393	0.7 , 2.5	0.0 , 500.0	C
	P2p1/2(Ox.Imp.)	133.6341	1.9679	GL(30)	48.43	16.70	C + 0.87	C^1	C^0.5	D
	P2p(PFSelectrolyte)	135.7906	2.4157	GL(30)	37.17	12.81	144.393 , 124.393	0.7 , 2.5	0.0 , 10000000.0	E
	P2p(PFSelectrolyte)	136.6306	2.4157	GL(30)	18.58	6.40	E + 0.87	E^1	E^0.5	F
VIII	P2p3/2(P=C)	129.9328	1.1539	GL(30)	57.56	19.71	131.543 , 129.543	0.7 , 1.5	0.0 , 10000000.0	A
	P2p1/2(P=C)	130.8028	1.1539	GL(30)	28.78	9.85	A + 0.87	A^1	A^0.5	B
	P2p3/2(Ox.Imp.)	132.7935	2.1645	GL(30)	105.85	36.23	144.543 , 124.543	0.7 , 2.5	0.0 , 500.0	C
	P2p1/2(Ox.Imp.)	133.6635	2.1645	GL(30)	52.93	18.11	C + 0.87	C^1	C^0.5	D
	P2p(PFSelectrolyte)	136.0150	1.7885	GL(30)	31.35	10.72	144.543 , 124.543	0.7 , 2.5	0.0 , 10000000.0	E
	P2p(PFSelectrolyte)	136.8850	1.7885	GL(30)	15.67	5.36	E + 0.87	E^1	E^0.5	F
IX	P2p3/2(P=C)	129.9066	1.2994	GL(30)	66.02	21.15	131.525 , 129.525	0.7 , 1.5	0.0 , 10000000.0	A
	P2p1/2(P=C)	130.7766	1.2994	GL(30)	33.01	10.57	A + 0.87	A^1	A^0.5	B
	P2p3/2(Ox.Imp.)	132.7881	2.0742	GL(30)	102.21	32.73	144.525 , 124.525	0.7 , 2.5	0.0 , 500.0	C
	P2p1/2(Ox.Imp.)	133.6581	2.0742	GL(30)	51.11	16.36	C + 0.87	C^1	C^0.5	D
	P2p(PFSelectrolyte)	135.9594	2.4134	GL(30)	39.98	12.79	144.525 , 124.525	0.7 , 2.5	0.0 , 10000000.0	E
	P2p(PFSelectrolyte)	136.8294	2.4134	GL(30)	19.99	6.40	E + 0.87	E^1	E^0.5	F

Table S2. Parameters and constraints used to fit C 1s, P 2p, and S 2p spectra of **1a (**I, II**), 2a (**III, IV**)**, and ***poly*-2a *(***V-IX*)* samples.

Table S3. Parameters and constraints used to fit C 1s, As 3d, and S 2p spectra of **1b (**I, II**), 2b (**III, IV**)**, and ***poly-*****2b (***V-VIII***)** samples.

a) ***poly-2a***

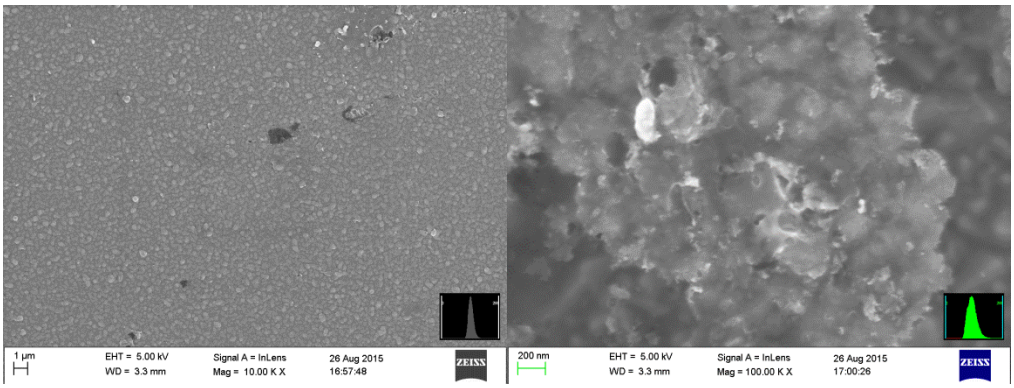

b) *poly-2b*

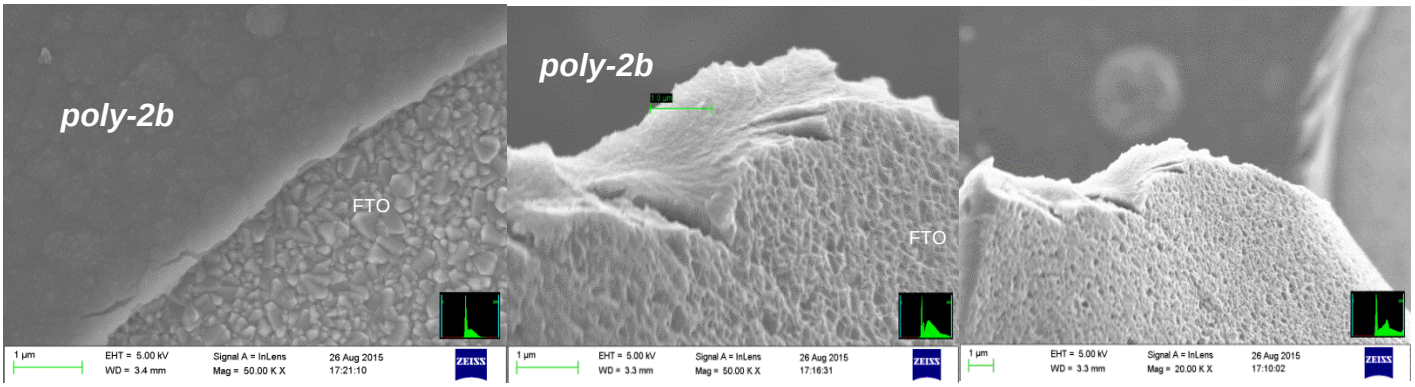

Figure S8. SEM pictures of ***poly-2a*** and ***poly-2b*** films; a) ***poly-2a*** b) ***poly-2b***.

a) ***poly*-2a**

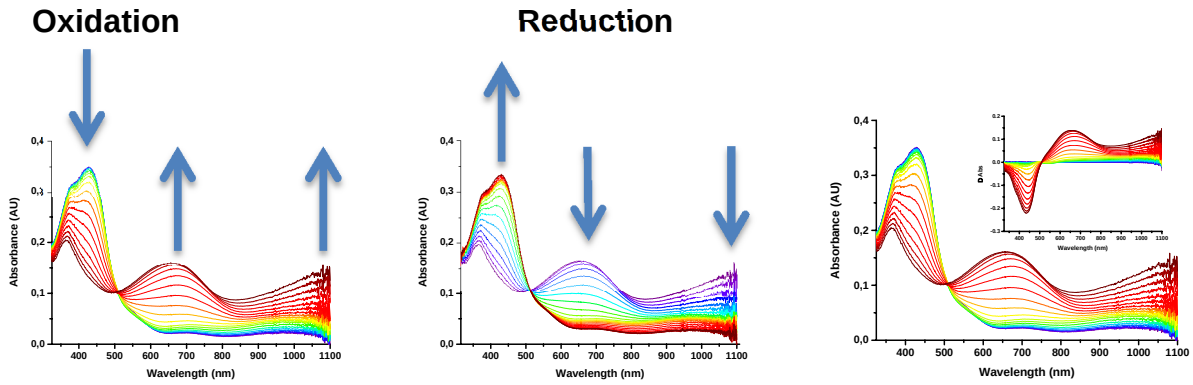

b) ***poly*-2b**

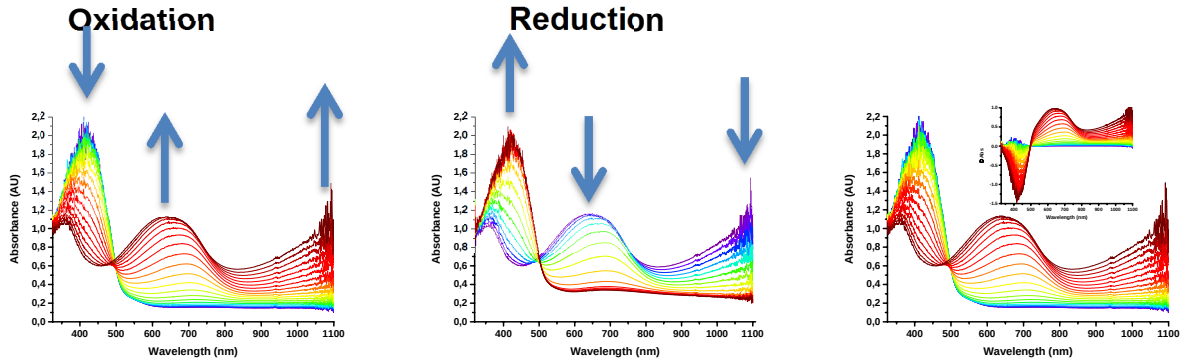

c)

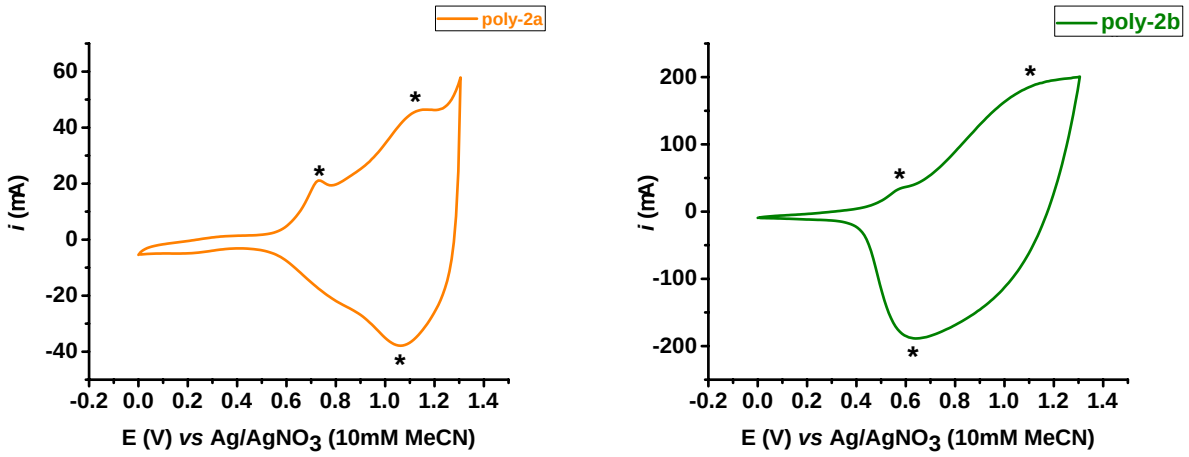

Species	Epa_1 (V) vs. $Ag/AgNO_3$ (10mM DCM)	Epa_2 (V) vs. $Ag/AgNO_3$ (10mM DCM)	$Epic$ (V) vs. $Ag/AgNO_3$ (10mM DCM)
poly-2a	0.73	1.20	1.06
poly-2b	0.57	1.07	0.64

d)

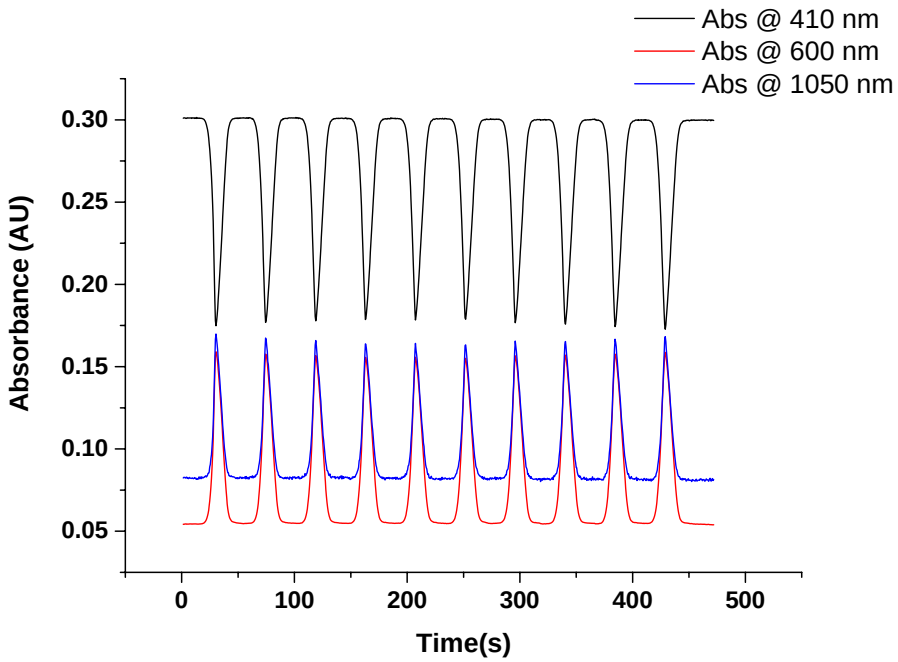

Figure S9. Spectro-electrochemistry of a) ***poly*-2a** and b) ***poly*-2b;** transparent DCM solution (0.1 mM *n*-Bu_4NPF_6); 0 to 1.3 V at a scan rate of 100 mV s^{-1}; inset: differential plot. c) Electrochemical response of poly-2a and poly-2b; transparent DCM solution (0.1 mM *n*-Bu_4NPF_6); asterisks indicate approximate positions for anodic and cathodic peak waves. d) Electrochromic reversibility of a sample of ***poly-2b*** at different selected absorption wavelengths for ~8 minutes (0 to 1.3 V at a scan rate of 100 mV s^{-1}).

a) b)

Neutral à Oxidized

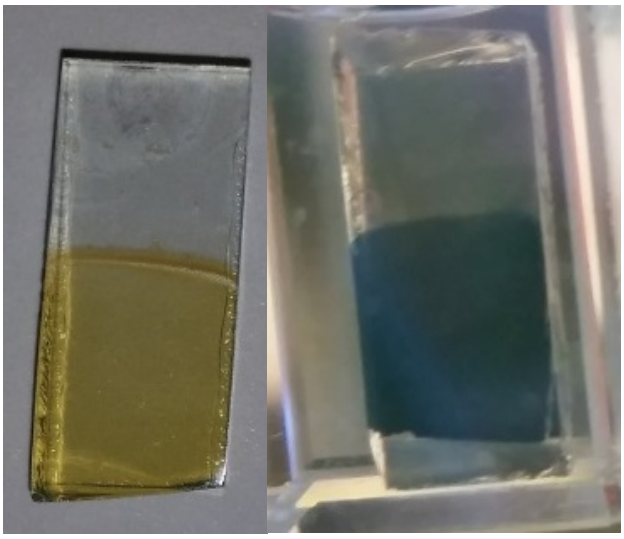

Figure S10. Pictures of a) neutral ***poly*-2b** and b) oxidized film of ***poly*-2b** with no applied bias under inert conditions**.**

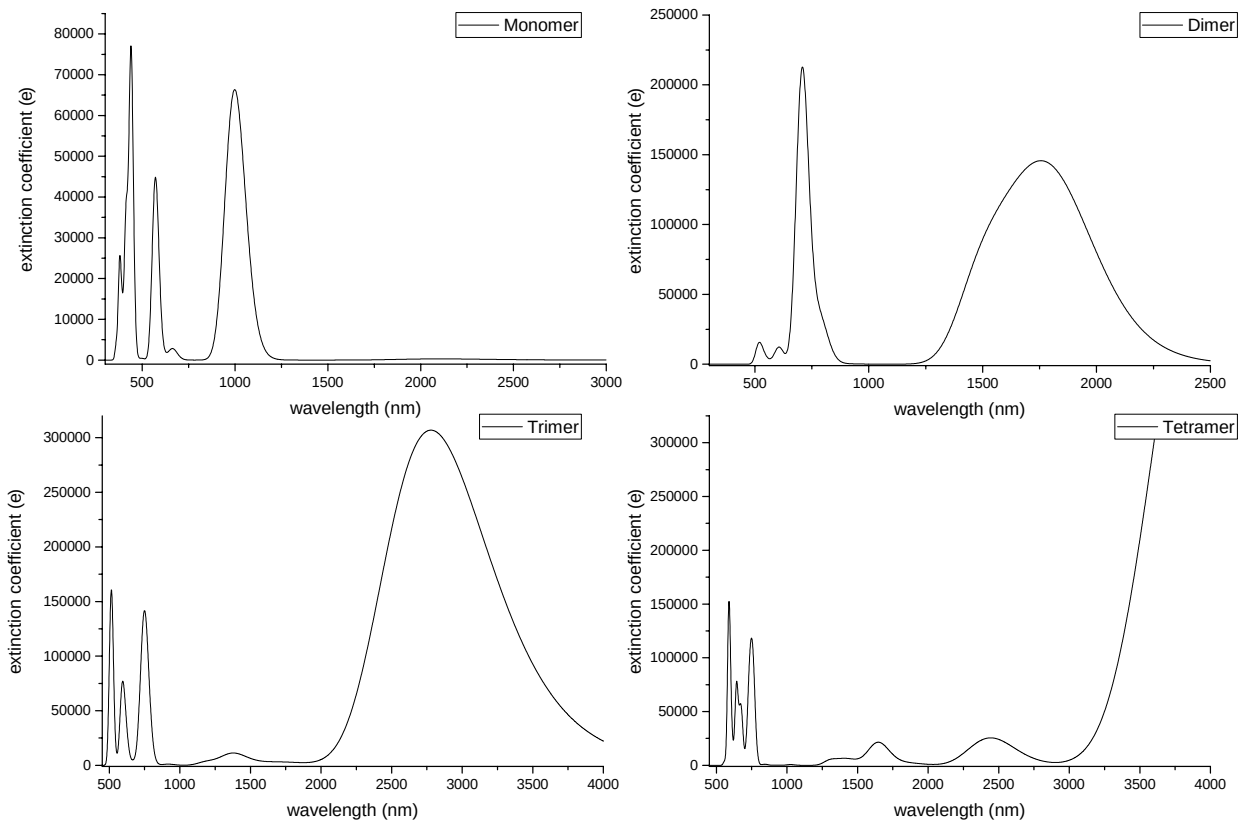

Figure S11. Simulated TD-DFT UV-Vis-NIR spectra of cations: **2b**$^{\bullet+}$, **2b**$^{\bullet+}$-dimer, **2b**$^{\bullet+}$-trimer, and **2b**$^{\bullet+}$-tetramer. Vertical lines indicate wavelength of electronic excitation, Intensity is in principle Oscillator Strength. Notice how the most intense bands for the monomer cation are in the visible and NIR region, whereas the most intense bands for oligomeric cations are located in the red-NIR and IR region in accordance to the spectro-electrochemistry of ***poly*-2a** and ***poly*-2b.**

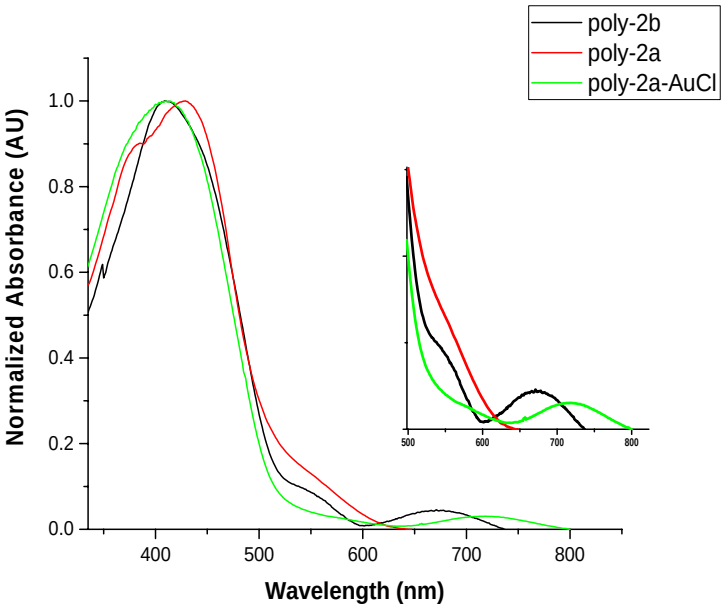

Figure S12. UV-Vis spectra of solid ***poly*-2a**, ***poly*-2b** and **poly-2a-AuCl** on a FTO-doped glass substrate.

a)

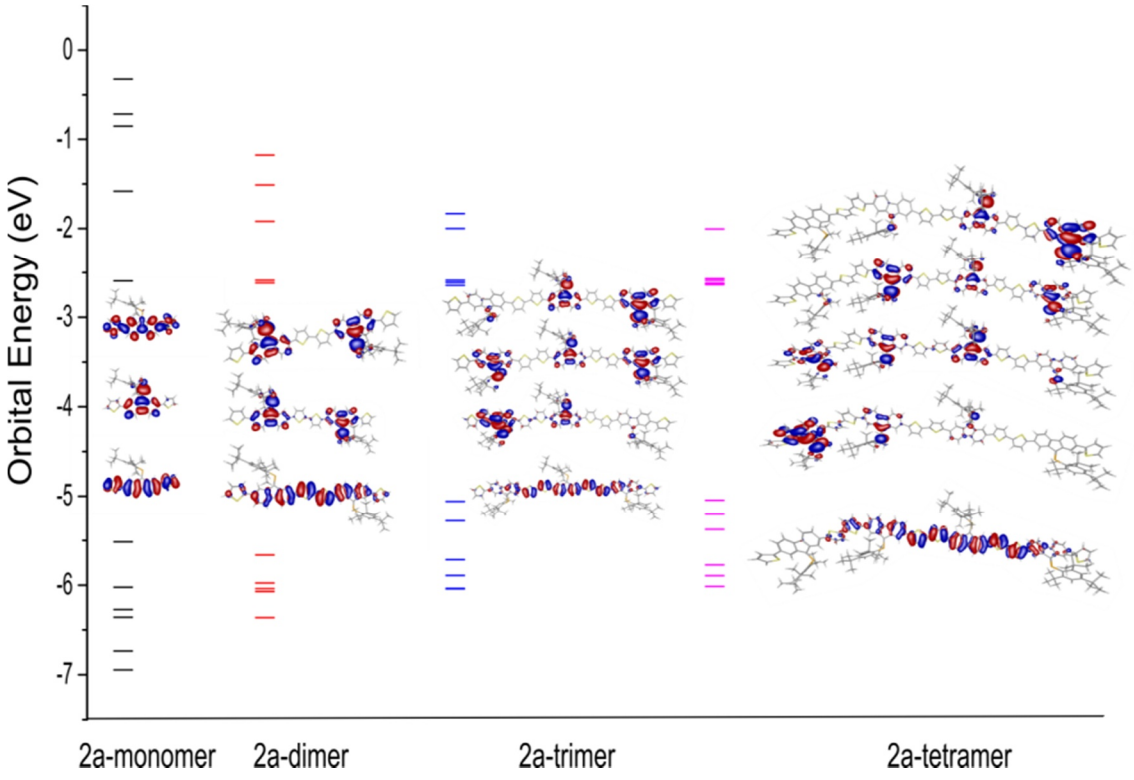

b)

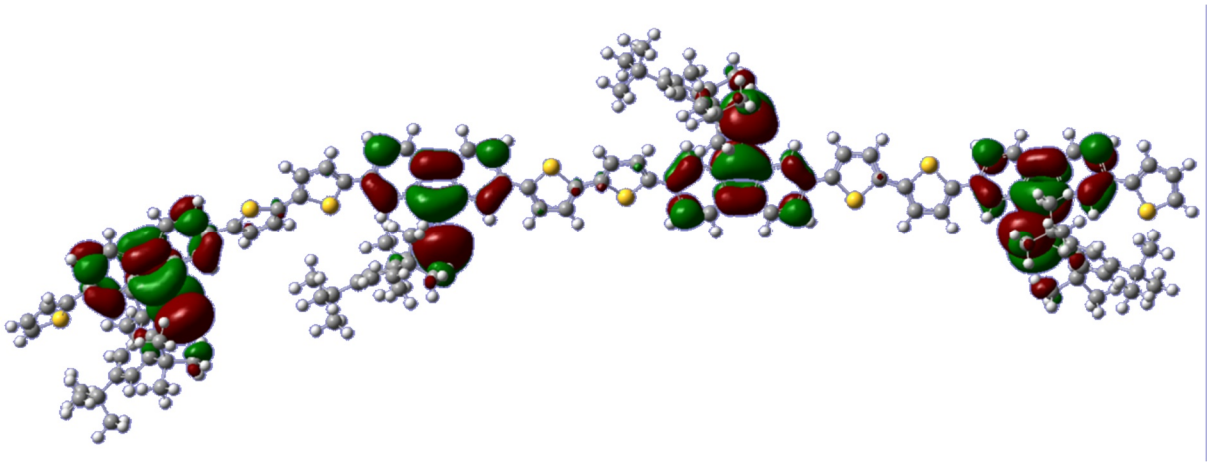

Figure S13. Selected DFT pictures of a) **2a, 2a**-dimer, **2a**-trimer, and **2a**-tetramer; Isosurface value: 0.02 a.u. For **2b**, see main manuscript b) The linear combination of LUMO to LUMO+3, which exemplifies the electronic structure of **poly-2b,** pointing toward an efficient lowering of the unoccupied band by incorporating the pnictogen-containing heterofulvene moiety.

Species	**HOMO-LUMO gap (eV)**	**Species**	**HOMO-LUMO gap (eV)**
2b	2.78	2a	2.92
2b-dimer	2.37	2a-dimer	2.51
2b-trimer	2.28	2a-trimer	2.42
2b-tetramer	2.26	2a-tetramer	2.41

Table S4. DFT calculated HOMO-LUMO gaps of monomers and oligomers.

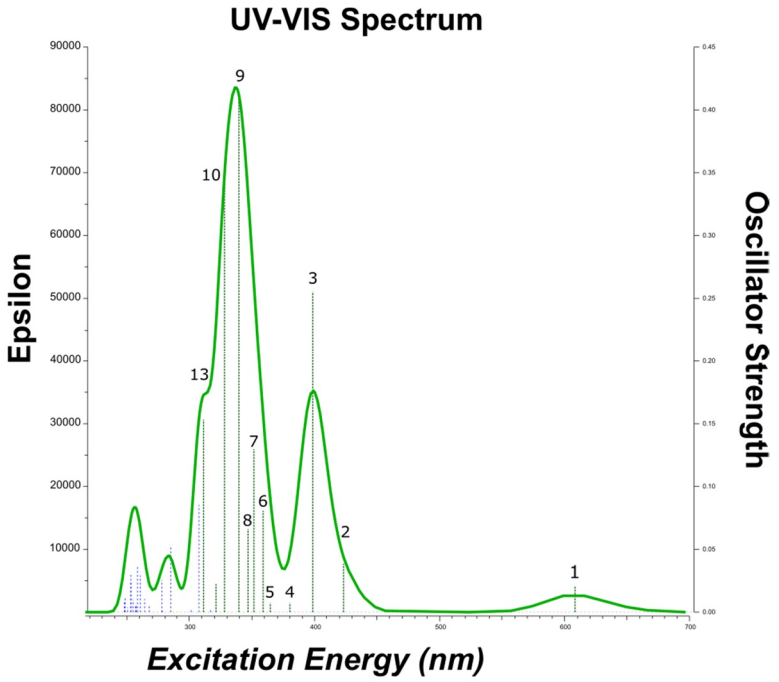

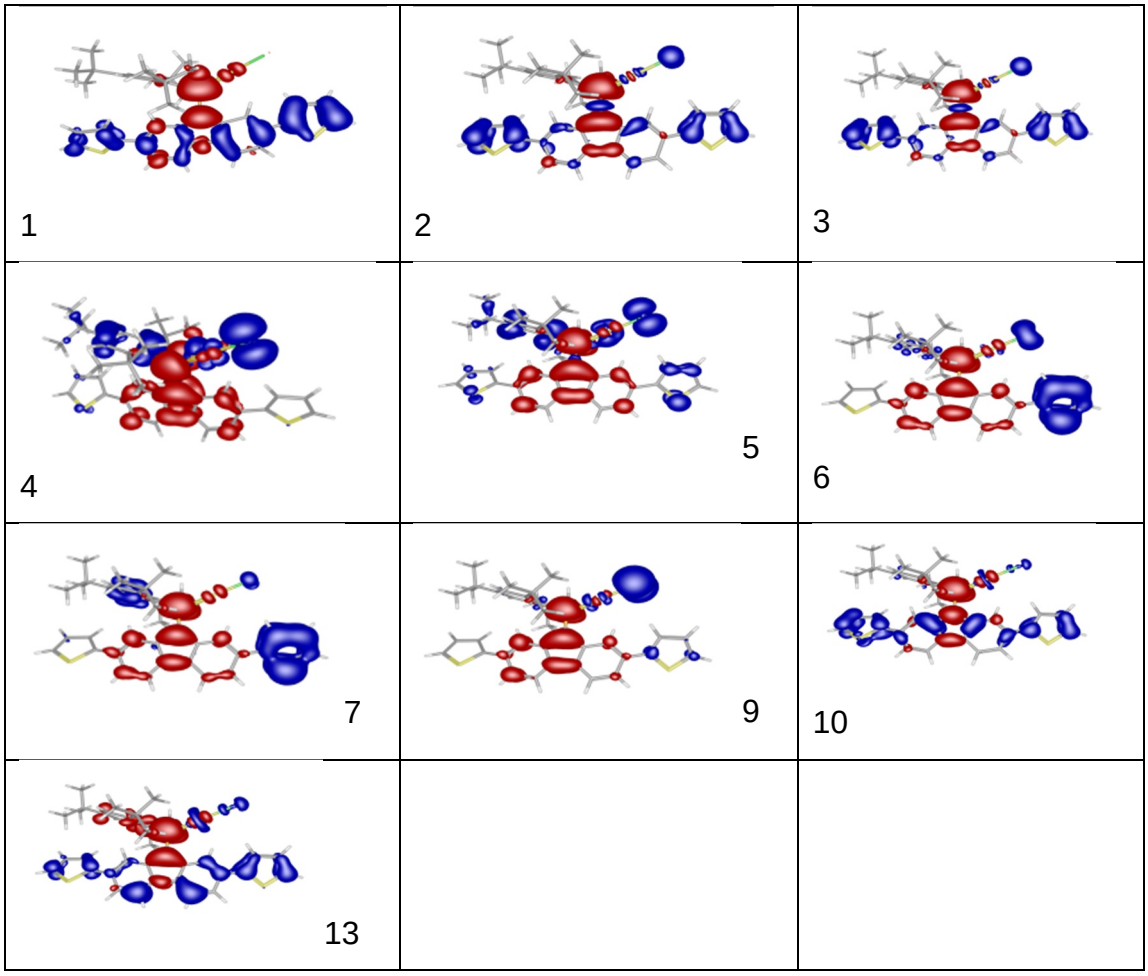

Figure S14. Calculated UV-Vis spectra of **2a-Au** using time-dependent DFT at the PBE1PBE using the LANL2DZ basis set for gold (Au) and 6-311G** on other atoms; numbers above vertical lines

indicate number of transition; blue: decrease of electron density, red: increase of electron density. b) **2a-Au** EDDM plots for transitions 1, 2, 3, 4, 5, 6, 7, 9, 10, and 13; left to right, top to bottom.

Species	λ_{onset} (nm)	Optical Gap (eV)
2a	552	2.25
2a-AuCl	648	1.91
***poly*-2a**	647	1.92
***poly*-2a-AuCl**	800	1.55
2b	596	2.08
***poly*-2b**	737	1.68

Table S5. A) λ_{onset} (nm) and Optical Gaps (eV) of all synthesized species, calculated according to literature procedures.[12]

1b ^{1}H-NMR Spectrum

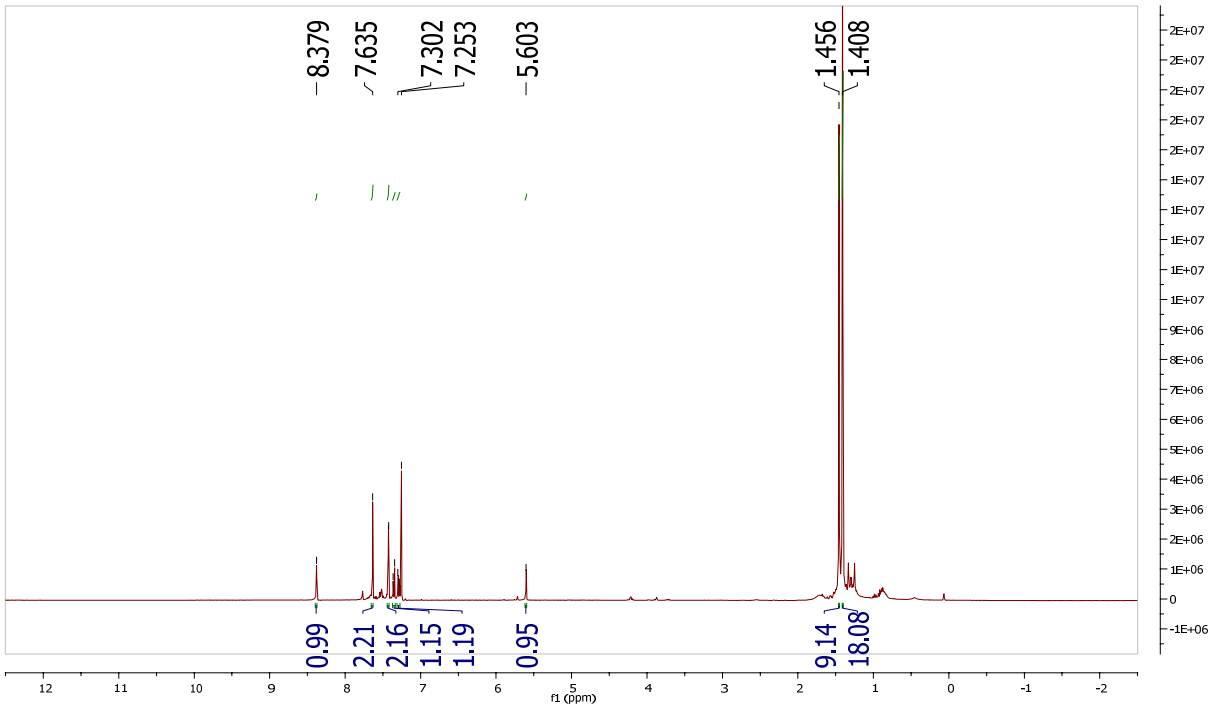

1b ^{13}C-NMR Spectrum

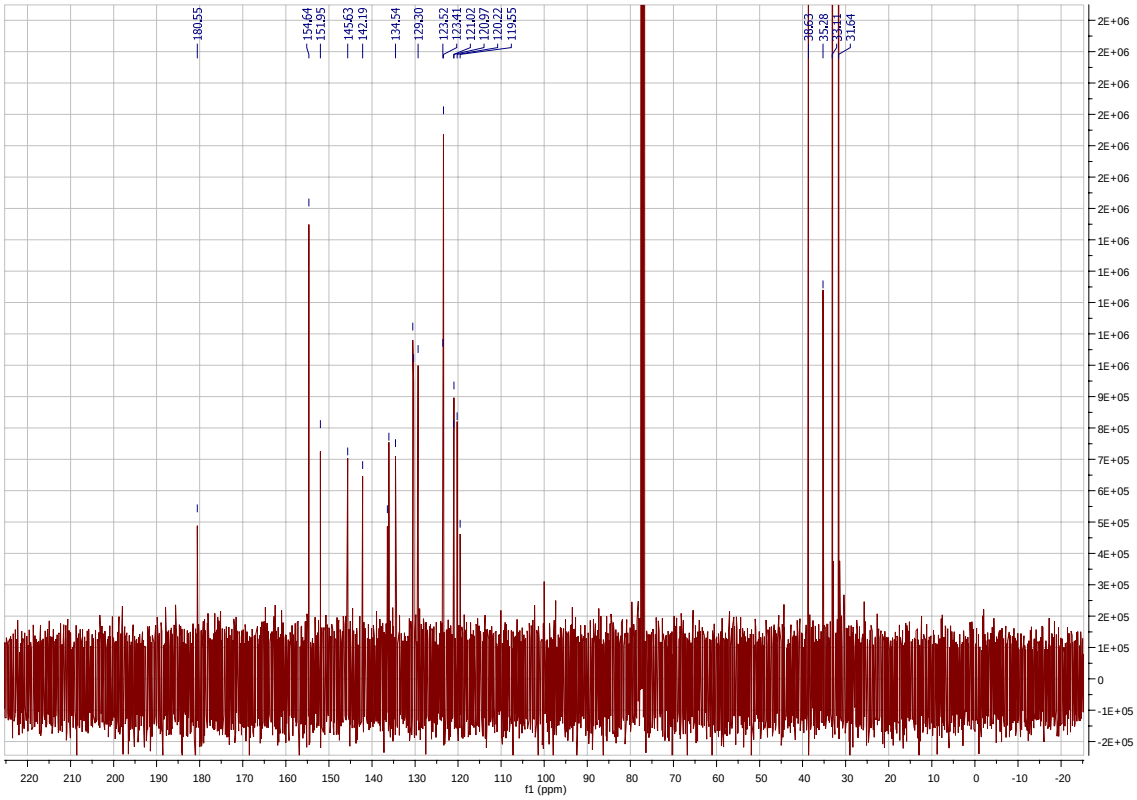

2b ^{1}H-NMR Spectrum

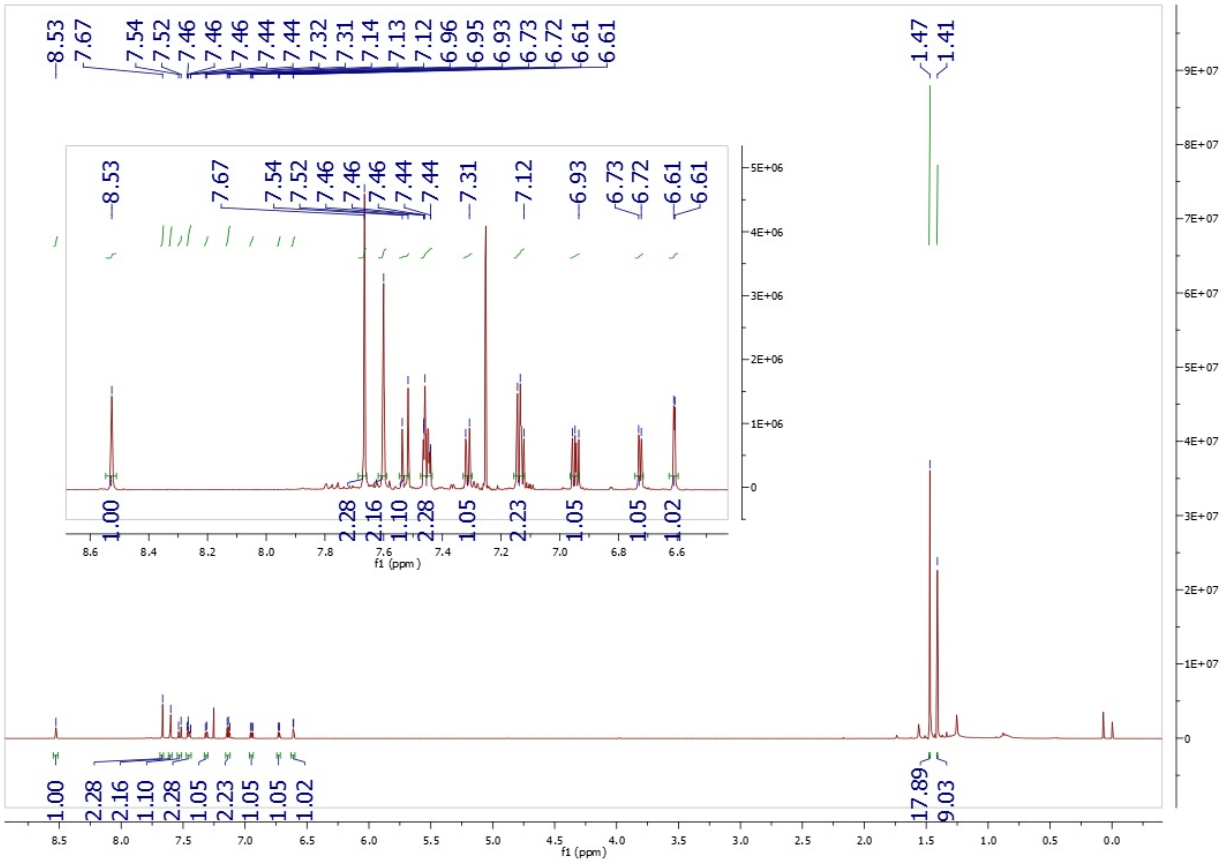

2b ^{13}C-NMR Spectrum

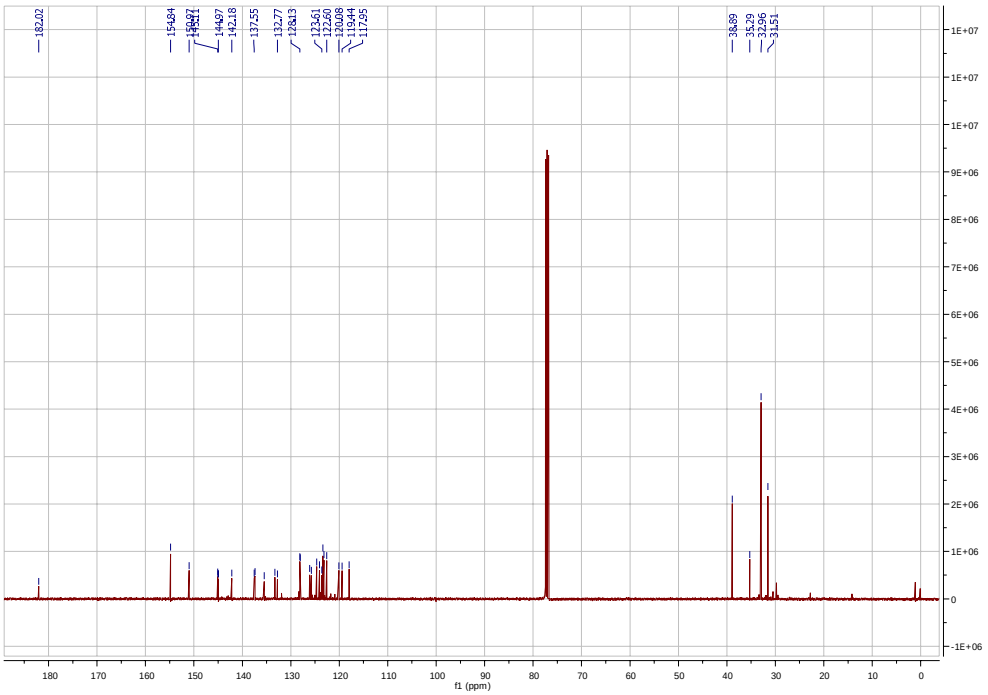

a ^{1}H-NMR Spectrum

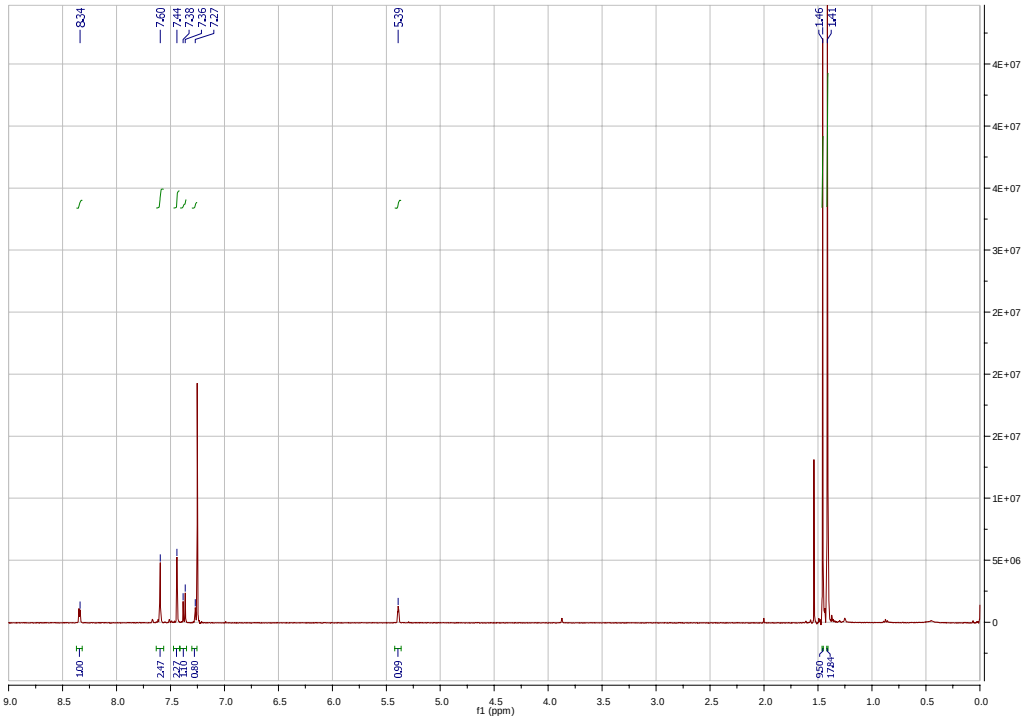

1a ^{13}C-NMR

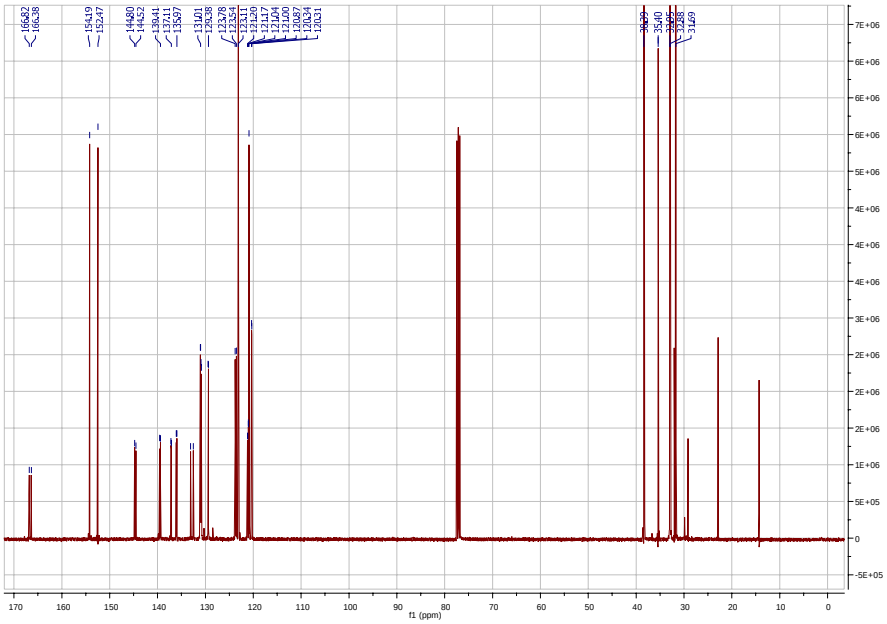

1a expansions of ^{13}C spectra.

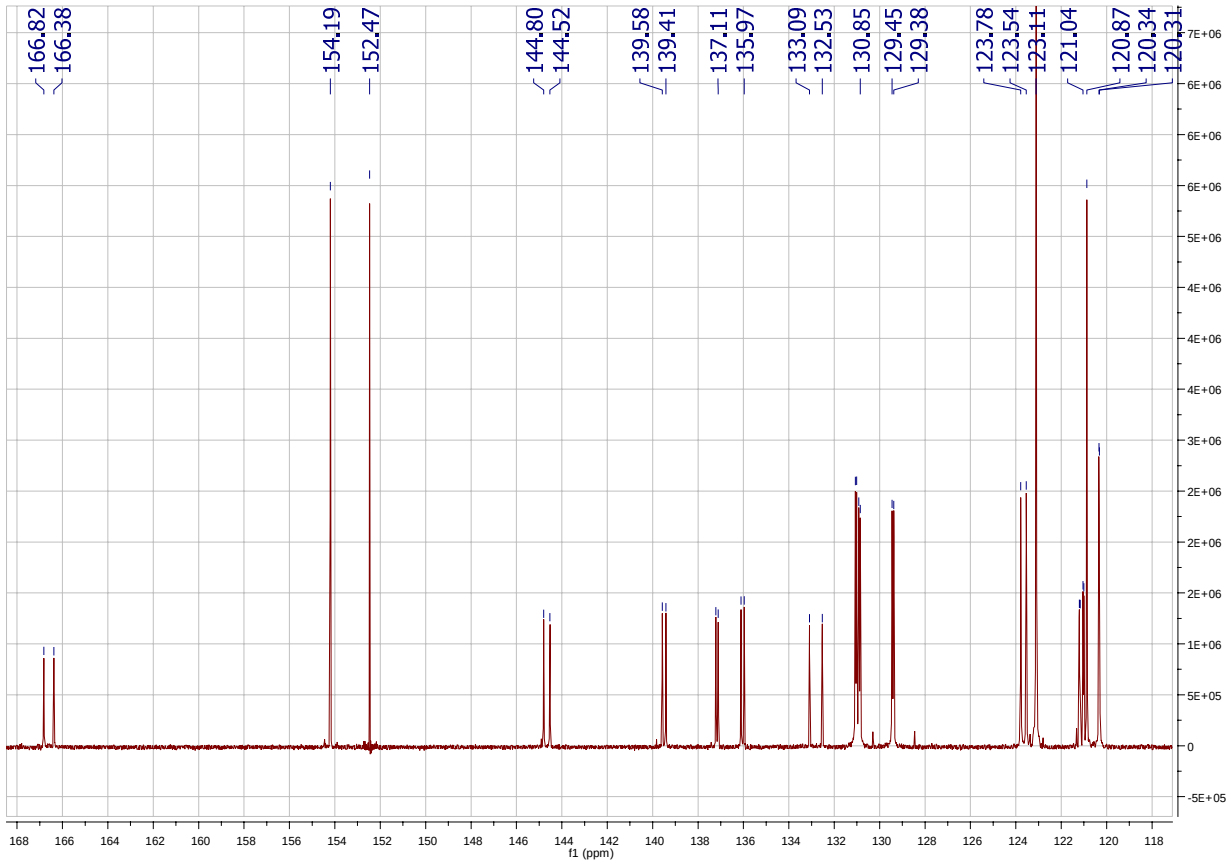

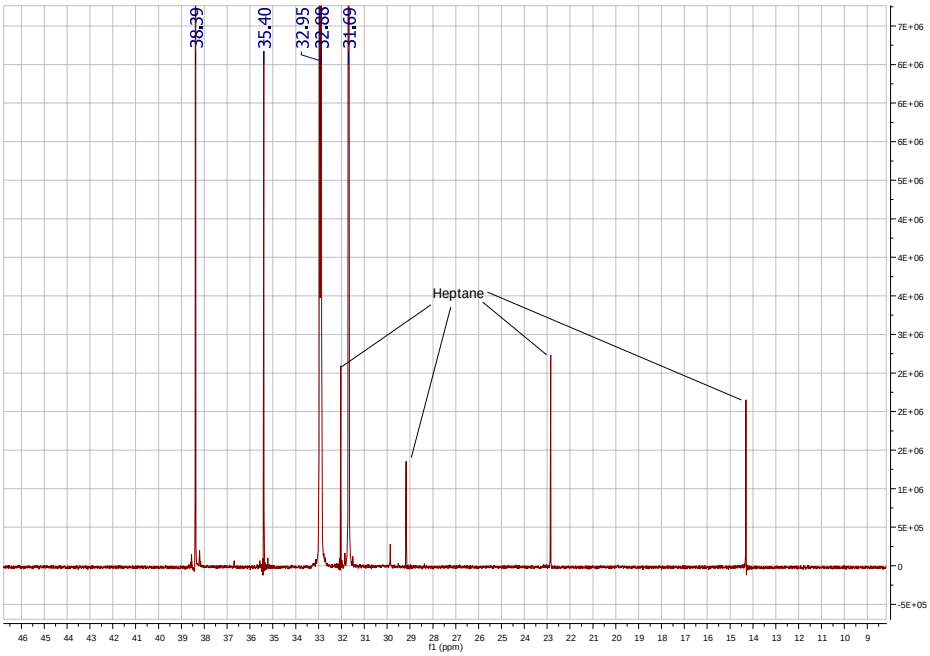

1a ^{31}P-NMR

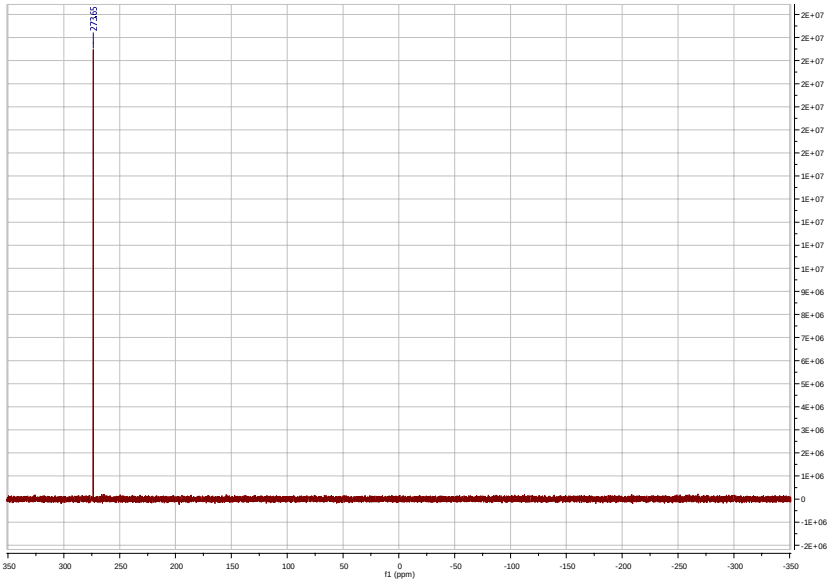

2a ^{1}H NMR spectrum

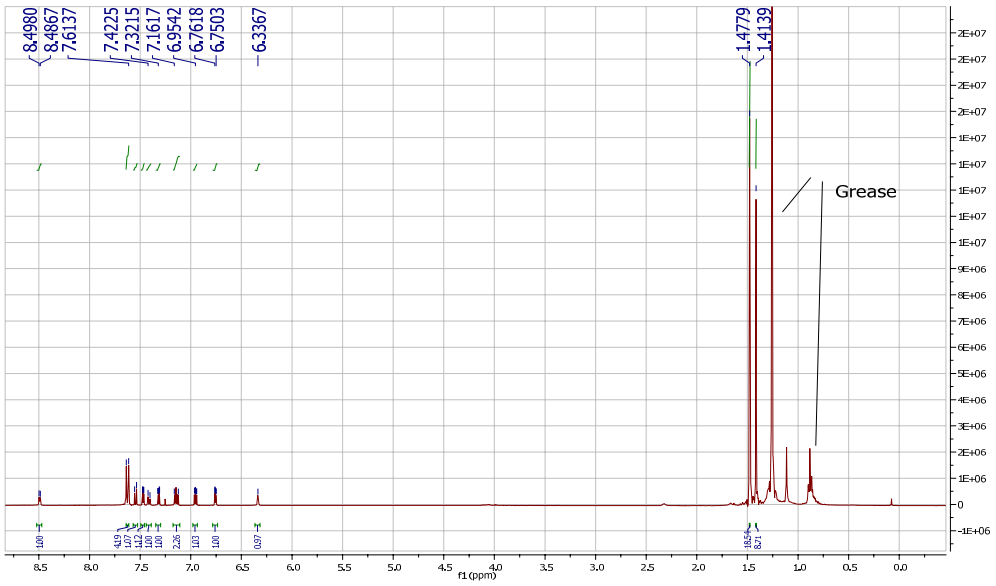

2a ^{13}C NMR spectrum

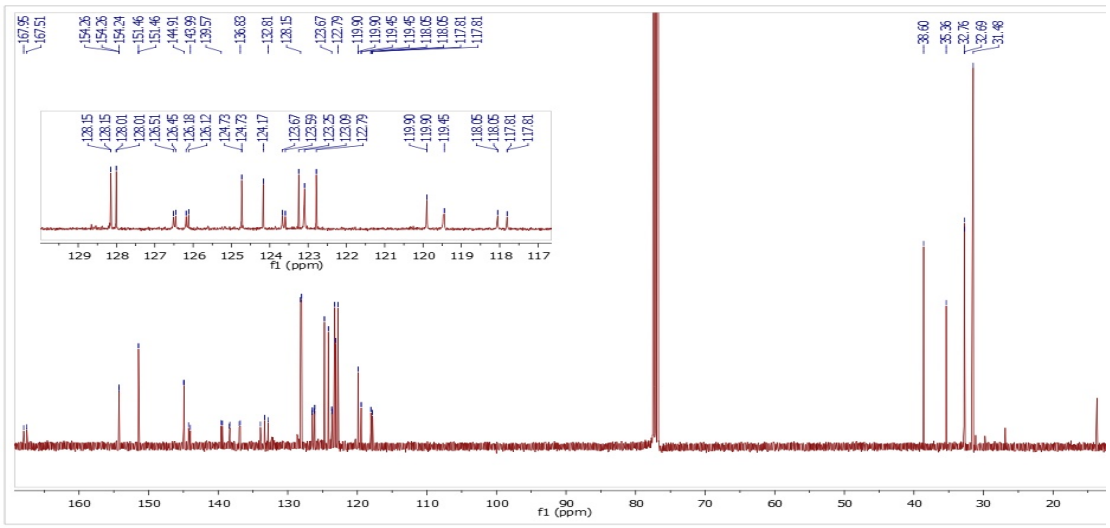

2a ^{31}P NMR spectrum

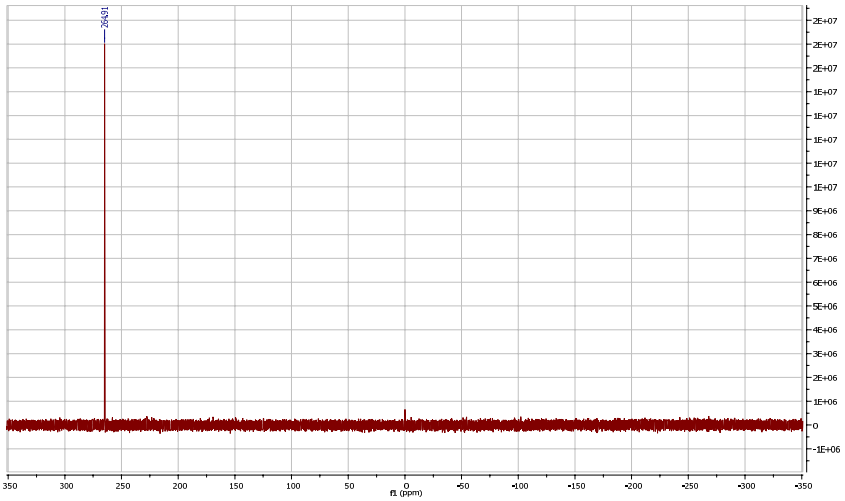

2a-Au ^{1}H NMR spectrum

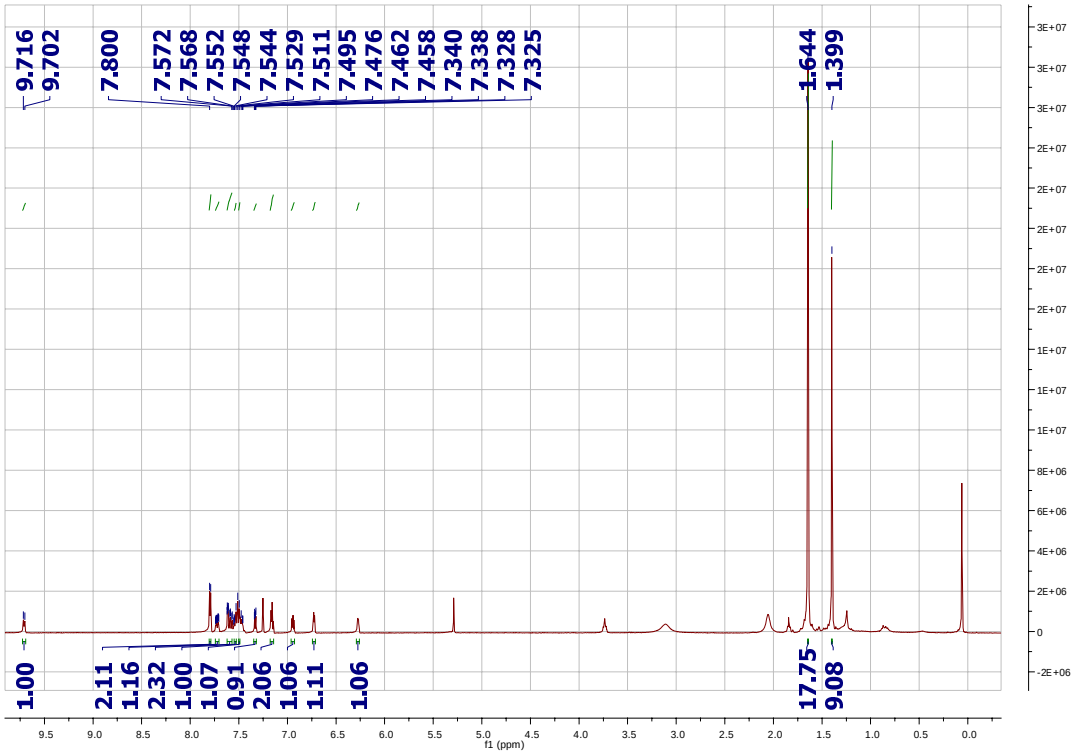

2a-Au ^{13}C NMR spectrum

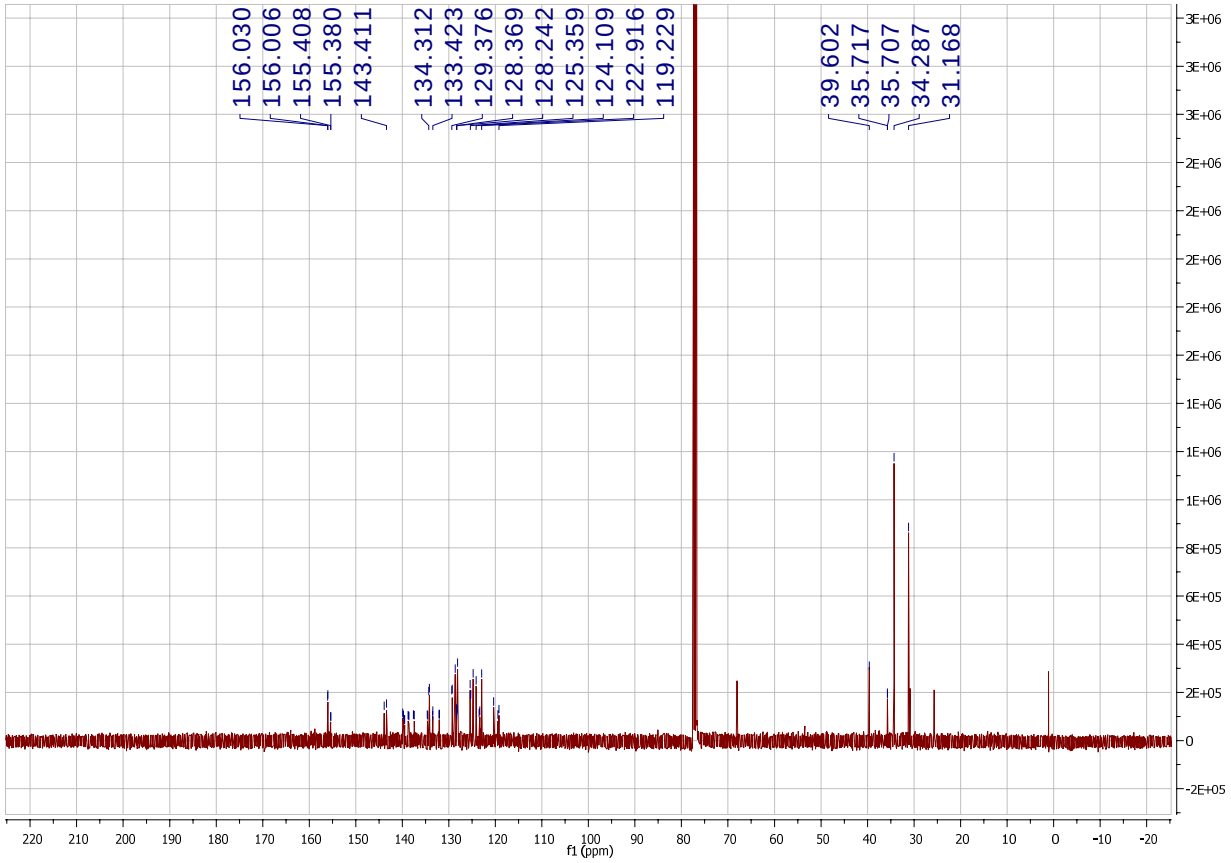

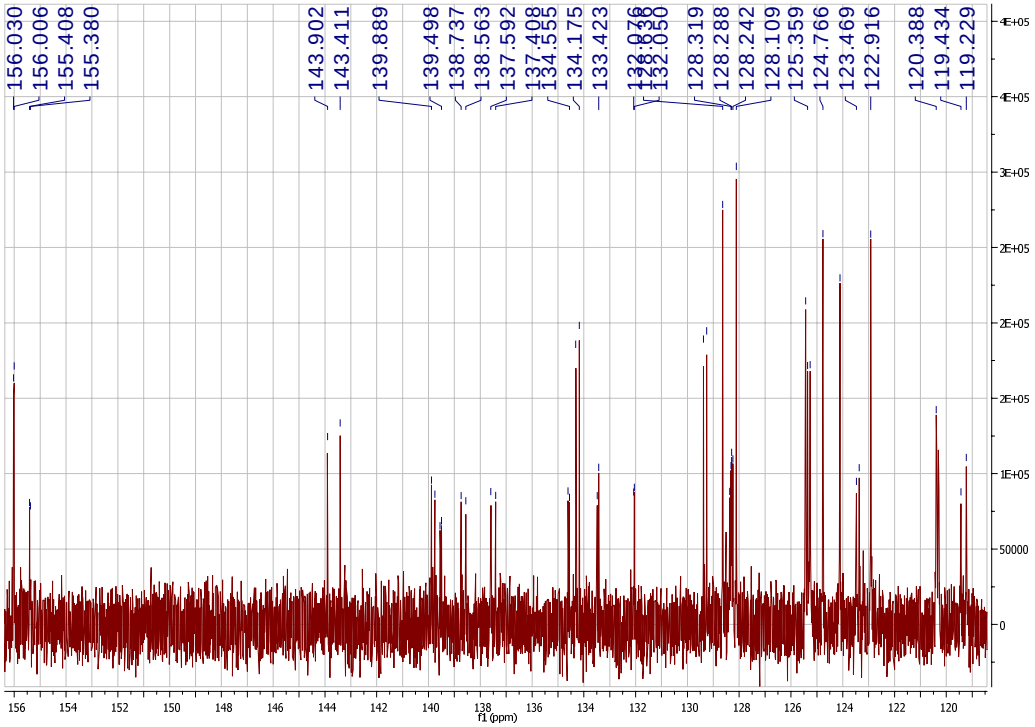

2a-Au ^{31}P NMR spectrum

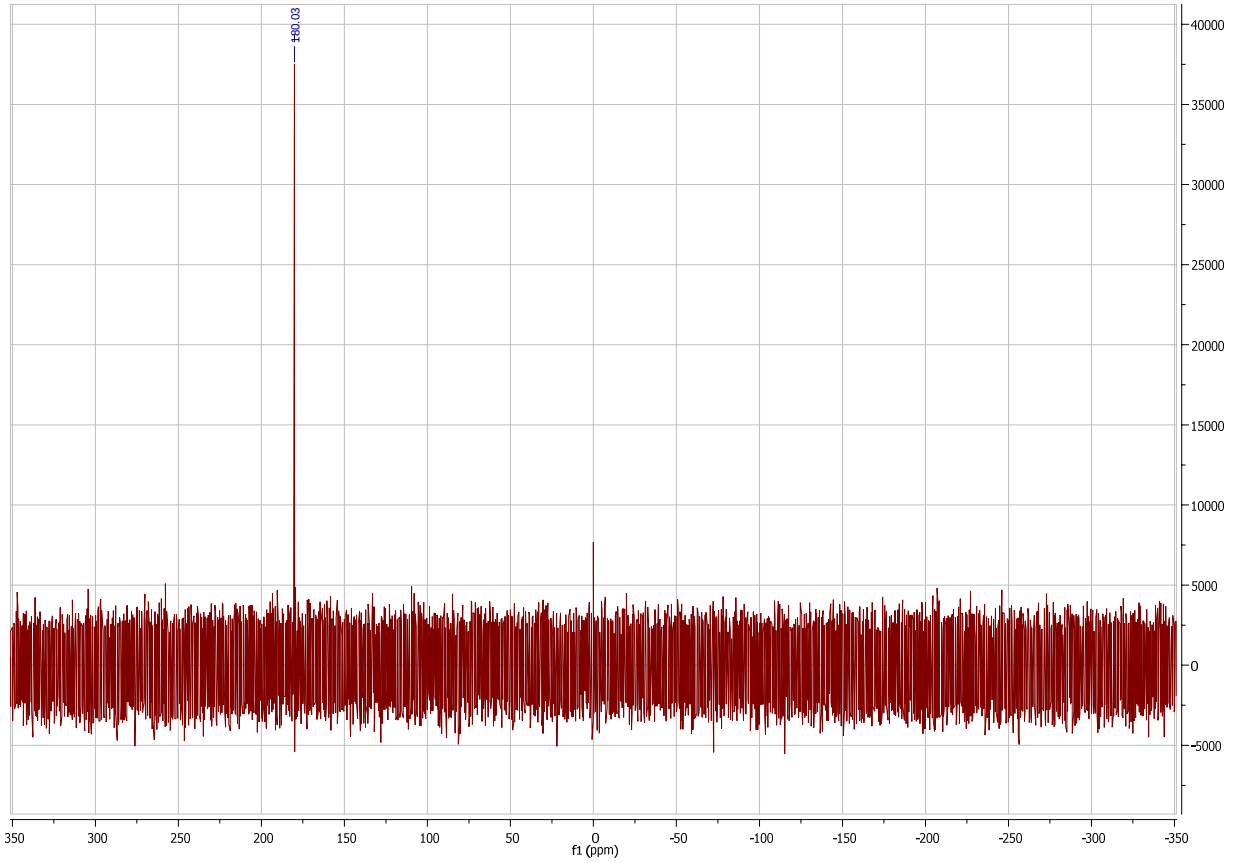

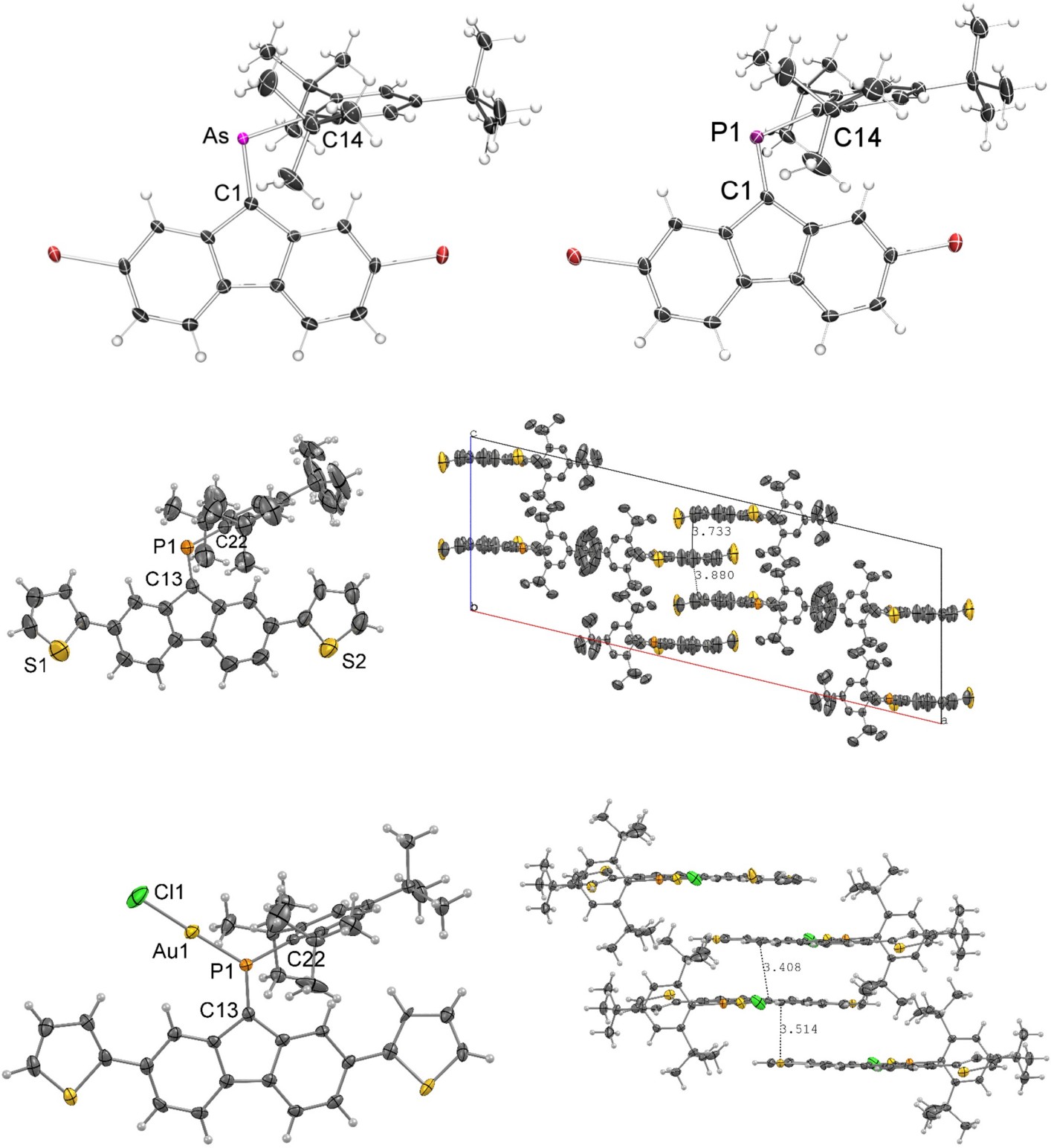

Figure S15. ORTEP plots of X-ray structure of **1a** (top left) and **1b** (top right) and **2a** (middle) and **2a-AuCl** (bottom). Probability ellipsoids are drawn at 50%. Selected bond lengths [Å] and angles [°]: **1a**: P1-C1 1.693(5), P1-C14 1.836(5), C1-P1-C14 104.0(2). **1b**: As1-C1 1.807(3), As1-C14 1.970(3), C1-As1-C14 102.6(1). **2a**: P1-C13 1.677(5), P1-C22 1.844(4), C13-P1-C14 108.4(2) Packing motif along the b axis (010) revealing short (< 3.9 Å) intermolecular distances between fluorene moieties **2a-AuCl**: P1-C13 1.665(5), P1-Au1 2.2144(13), P1-C22 1.810(5), C13-P1-C22 112.8(2). Intermolecular packing showing short distances between the π-systems (3.51 and 3.41 Å).

Crystal data	**1a**	**1b**
CCDC-No.	1431893	1431892
Empirical formula	$C_{31}H_{35}Br_2P$	$C_{31}H_{35}AsBr_2$
Formula weight	598.38	642.33
Crystal description	Orange-yellow block	Orange block
Crystal size	0.22 x 0.20 x 0.17	0.26 x 0.20 x 0.13
Crystal system, space group	Monoclinic P $2_1/c$	Monoclinic P $2_1/c$
Unit cell dimensions: a	10.1490(8)	10.1345(5)
b	23.497(2)	23.5740(11)
c	11.9741(11)	12.0357(6)
α	90	90
β	105.805(6)	105.189(2)
γ	90	90
Volume	2747.5(4)	2775.0(2)
Z	4	4
Calculated density	1.447 Mg/m³	1.537 Mg/m³
F(000)	1224	1296
Linear absorption coefficient μ	3.027 mm^{-1}	4.122 mm^{-1}
Absorption correction	multi-scan, SADABS 2008	multi-scan, SADABS 2008
Max. and min. transmission	0.4840 and 0.7454	0.4146 and 0.7457
Unit cell determination	1.7 < Q < 25.2°	1.7 < Q < 25.2°
	3889 reflections used at 100K	4876 reflections used at 100K
Data collection		
Temperature	100(2)K	
Diffractometer	Bruker APEX-II CCD	
Radiation source	fine-focus sealed tube	
Radiation and wavelength	MoK_a, 0.71073Å	
Monochromator	Graphite	
Scan type	w scans	
Q range for data collection	1.7 < Q < 26.6°	1.7 < Q < 28.6°
Index ranges	-12 £ h £ 12, -29 £ k £ 28, -15 £ l £ 13	-12 £ h £ 13, -31 £ k £ 27, -16 £ l £ 16
Reflections collected / unique	20787/ 5692	24799 / 6931
Significant unique reflections	3889 with I > 2s(I)	4876 with I > 2s(I)
R(int), R(sigma)	0.0849, 0.0848	0.0717, 0.0594
Completeness to Q_{max}	99.3%	99.8%
Refinement		
Refinement method	Full-matrix least-squares on F^2	
Data / parameters / restraints	5692/ 316/ 0	6931 / 316 / 0
Goodness-of-fit on F^2	1.039	1.025
Final R indices [I > 2s(I)]	R1 = 0.0529, wR2 = 0.1061	R1 = 0.0423, wR2 = 0.0793
R indices (all data)	R1 = 0.0911, wR2 = 0.1186	R1 = 0.0772, wR2 = 0.0875
Weighting scheme	$w=1/[s^2(F_o^2)+(aP)^2+bP]$ where $P=(F_o^2+2F_c^2)/3$	
Weighting scheme parameters a	a = 0.0434, b = 3.0443	a = 0.0317, b = 1.6248
Largest D/s in last cycle	0.001	0.001
Largest difference peak and hole	0.829 and -0.723e/Å³	0.571 and -0.596 e/Å³
Structure Solution Program	SHELXS-2014 (Sheldrick, 2008)	SHELXS-2014 (Sheldrick, 2008)
Structure Refinement Program	SHELXL-2014 (Sheldrick, 2008)	SHELXL-2014/7 (Sheldrick, 2008)

Crystal data	**2a**	**2a-AuCl**
CCDC-No.	1485627	1486942
Empirical formula	$C_{39}H_{41}S_2P$	$C_{39}H_{41}AuClS_2P$
Formula weight	604.81	837.22
Crystal description	red prism	black block
Crystal size	0.48 x 0.38 x 0.35	0.38 x 0.20 x 0.09
Crystal system, space group	Monoclinic C 2/c	Monoclinic P $2_1/n$
Unit cell dimensions: a	40.116(4)	9.2061(3)
b	12.0063(11)	30.1345(10)
c	14.4519(16)	15.3956(5)
β	103.394(7)	105.096(2)
Volume	6771.4(12)	4123.7(2)
Z	8	4
Calculated density	1.187 Mg/m³	1.349 Mg/m³
F(000)	2576	1672
Linear absorption coefficient μ	0.230 mm^{-1}	3.795 mm^{-1}
Absorption correction	multi-scan, SADABS 2008	
Min. and max. transmission	0.6349 and 0.7454	0.4976 and 0.7455
Unit cell determination	1.0 < Q < 25.2°	1.9 < Q < 25.2°
	3953 reflections used at 100K	7626 reflections used at 100K
Data collection		
Temperature	297(3)K	100(2)K
Diffractometer	Bruker APEX-II CCD	
Radiation source	fine-focus sealed tube	
Radiation and wavelength	MoK_a, 0.71073Å	
Monochromator	Graphite	
Scan type	w scans	
Q range for data collection	1.0 < Q < 26.7°	1.9 < Q < 27.3°
Index ranges	-31 £ h £ 50, -14 £ k £ 15, -18 £ l £ 18	-11 £ h £ 11, -38 £ k £ 38, -19 £ l £ 19
Reflections collected / unique	32809/ 7077	71482/ 9229
Significant unique reflections	4007 with I > 2s(I)	7626 with I > 2s(I)
R(int), R(sigma)	0.0742, 0.0848	0.0434, 0.0648
Completeness to Q_{max}	99.9%	99.1%
Refinement details	The structure was refined with twinning along [010] and site occupation factors refined to approx. 0.21. The *para-tart*-butyl group was model with a positional disorder over two positions, however almost free rotation is observed which leads to large ellipsoids along the due to this rotation.	The structure was refined with a positional disorder of the two thiophene rings having sof's of 0.79 and 0.78. The ill-defined hexane molecule was treated by using the squeeze algorithm identifying solvent accessible voids (2x440 Å³) accounting for 2x 149 electrons. Further details can be found in the cif file.
Refinement method	Full-matrix least-squares on F^2	
Data / parameters / restraints	7077/ 408/ 36	9229/ 441/ 12
Goodness-of-fit on F^2	1.031	1.155
Final R indices [I > 2s(I)]	R1 = 0.0986, wR2 = 0.2790	R1 = 0.0478, wR2 = 0.0964
R indices (all data)	R1 = 0.1571, wR2 = 0.3216	R1 = 0.0619, wR2 = 0.1003
Weighting scheme	$w=1/[s^2(F_o^2)+(aP)^2+bP]$ where $P=(F_o^2+2F_c^2)/3$	
Weighting scheme parameters a	a = 0.1703, b = 12.5064	a = 0.022, b = 18.9161
Largest D/s in last cycle	0.001	0.002
Largest difference peak and hole	0.662 and -0.944 e/Å³	1.299 and -2.590 e/Å³
Structure Solution Program	SHELXS-2014 (Sheldrick, 2008)	
Structure Refinement Program	SHELXL-2014 (Sheldrick, 2008)	

References

[1] *Unpublished Work*.

[2] J. G. Rodríguez, J. L. Tejedor, T. La Parra, C. Díaz, *Tetrahedron* 2006, *62*, 3355-3361.

[3] D. Briggs, *Surface analysis of polymers by XPS and static SIMS*, Cambridge University Press, 1998.

[4] R. Haerle, E. Riedo, A. Pasquarello, A. Baldereschi, *Phys. Rev. B* 2001, *65*, 045101.

[5] A. Lachkar, A. Selmani, E. Sacher, *Synthetic Metals* 1995, *72*, 73-80.

[6] X. L. Wei, M. Fahlman, A. J. Epstein, *Macromolecules* 1999, *32*, 3114-3117.

[7] a) A. M. Botelho do Rego, A. M. Ferraria, J. El Beghdadi, F. Debontridder, P. Brogueira, R. Naaman, M. Rei Vilar, *Langmuir* 2005, *21*, 8765-8773; b) D. Skomski, S. L. Tait, *The Journal of Physical Chemistry C* 2014, *118*, 1594-1601.

[8] A. J. Nelson, S. Glenis, A. J. Frank, *J. Chem. Phys* 1987, *87*, 5002-5006.

[9] S. Hofmann, *Auger- and X-Ray Photoelectron Spectroscopy in Materials Science: A User-Oriented Guide*, Springer Berlin Heidelberg, 2012.

[10] J. Li, X. Gao, B. Liu, Q. Feng, X.-B. Li, M.-Y. Huang, Z. Liu, J. Zhang, C.-H. Tung, L.-Z. Wu, *J. Am. Chem. Soc.* 2016.

[11] A. Kim, F. S. Ou, D. A. A. Ohlberg, M. Hu, R. S. Williams, Z. Li, *J. Am. Chem. Soc.* 2011, *133*, 8234-8239.

[12] a) S. Rasmussen, in *Encyclopedia of Polymeric Nanomaterials* (Eds.: S. Kobayashi, K. Müllen), Springer Berlin Heidelberg, Berlin, Heidelberg, 2014, pp. 1-13; b) J.-L. Bredas, *Materials Horizons* 2014, *1*, 17-19.